

Nuclear spin structure in dark matter search: The finite momentum transfer limit

V.A. Bednyakov

*Dzhelepov Laboratory of Nuclear Problems, Joint Institute for Nuclear Research,
141980 Dubna, Russia; E-mail: Vadim.Bednyakov@jinr.ru*

and F. Šimkovic

*Department of Nuclear Physics, Comenius University,
Mlynská dolina F1, SK-842 15 Bratislava, Slovakia*

(Dated: October 5, 2018)

Spin-dependent elastic scattering of weakly interacting massive dark matter particles (WIMP) off nuclei is reviewed. All available, within different nuclear models, structure functions $S(q)$ for *finite* momentum transfer ($q > 0$) are presented. These functions describe the recoil energy dependence of the differential event rate due to the spin-dependent WIMP-nucleon interactions. This paper, together with the previous paper “Nuclear spin structure in dark matter search: The zero momentum transfer limit”, completes our review of the nuclear spin structure calculations involved in the problem of direct dark matter search.

PACS: 95.35.+d, 12.60.Jv, 14.80.Ly

Keywords: weak-interacting massive particle, supersymmetry, neutralino, nuclear matrix element

I. INTRODUCTION

Weakly Interacting Massive Particles (WIMPs) are among the most popular candidates for the relic cold dark matter (DM). There is some revival of interest in the WIMP-nucleus spin-dependent interaction from both theoretical (see e.g. [1, 2, 3, 4, 5, 6, 7, 8]) and experimental (see e.g. [9, 10, 11, 12, 13, 14, 15, 16, 17, 18, 19]) points of view. There are some proposals aimed at direct DM detection with relatively low-mass isotope targets [9, 10, 15, 16, 17, 18] as well as some attempts to design and construct a DM detector which is sensitive to the nuclear recoil direction [20, 21, 22, 23, 24, 25, 26]. Low-mass targets make preference for the low-mass WIMPs and are more sensitive to the spin-dependent WIMP-nucleus interaction as well [1, 3, 4, 7, 27, 28, 29]. On the other hand, WIMPs with masses about $100 \text{ GeV}/c^2$ follow from the results of the Dark Matter (DAMA) experiment. This collaboration claimed observation of the first evidence for the dark matter signal due to registration of the annual modulation effect [30, 31, 32]. Aimed for more than one decade at the DM particle direct detection, the DAMA experiment with 100-kg highly radio-pure NaI(Tl) scintillator detectors successfully operated

till July 2002 at the Gran Sasso National Laboratory of the I.N.F.N. On the basis of the results obtained for over 7 annual cycles (107731 kg-day total exposure) the effectiveness of the WIMP model-independent annual modulation signature was demonstrated and the WIMP presence in the galactic halo is strongly supported at 6.3σ C.L. [31].

The goal of this review (being a continuation of our previous review paper [7]) is to complete our nuclear physics consideration of the spin-dependent (or axial-vector) interaction of dark matter particles with nuclei. This type of interaction of the DM particles is important for the following reasons: (i) the spin-dependent interaction of the DM particles provides us with twice stronger constraints on the SUSY parameter space in comparison with the spin-independent interaction; (ii) in the case of spin-dependent interaction of heavy WIMPs with heavy target nuclei the so-called long q -tail behavior of the relevant form-factor allows detection of large nuclear recoil energy due to some nuclear structure effects; (iii) it is worthwhile to note that by relying only upon the scalar interaction of the DM particles, which seems to be strongly suppressed, one might miss a DM signal [4]. However, by a simultaneous study of both spin-dependent and spin-independent interactions of the DM particles with nuclei the chance for observing the DM signal is significantly increased.

A dark matter event is elastic scattering of a relic WIMP (or neutralino) χ with mass m_χ from a target nucleus A producing a nuclear recoil E_R which can be detected by a suitable detector. The differential event rate in respect to the recoil energy is the subject of experimental measurements. The rate depends on the distribution of the relic WIMPs in the solar vicinity $f(v)$ and the cross section of WIMP-nucleus elastic scattering [27, 29, 33, 34, 35, 36, 37, 38]. The differential event rate per unit mass of the target material has the form

$$\frac{dR}{dE_R} = N_T \frac{\rho_\chi}{m_\chi} \int_{v_{\min}}^{v_{\max}} dv f(v) v \frac{d\sigma^A}{dq^2}(v, q^2). \quad (1)$$

We assume WIMPs (neutralinos) to be a dominant component of the DM halo of our galaxy with a density $\rho_\chi = 0.3 \text{ GeV/cm}^3$ in the solar vicinity. The nuclear recoil energy $E_R = q^2/(2M_A)$ is typically about $10^{-6}m_\chi$ and N_T is the number density of a target nuclei with mass M_A . The WIMP-nucleus differential elastic scattering cross section for spin-non-zero ($J \neq 0$) nuclei contains coherent (spin-independent, or SI) and axial (spin-dependent, or SD) terms [1, 39, 40]:

$$\frac{d\sigma^A}{dq^2}(v, q^2) = \frac{d\sigma_{\text{SD}}^A}{dq^2}(v, q^2) + \frac{d\sigma_{\text{SI}}^A}{dq^2}(v, q^2) = \frac{S_{\text{SD}}^A(q^2)}{v^2(2J+1)} + \frac{\sigma_{\text{SI}}^A(0)}{4\mu_A^2 v^2} F_{\text{SI}}^2(q^2). \quad (2)$$

Here $\mu_A = \frac{m_\chi M_A}{m_\chi + M_A}$ is the reduced WIMP-nucleus mass, $\sigma_{\text{SI}}^A(0) = \frac{\mu_A^2}{\pi} [A^2 C_0^2]$ is the spin-independent WIMP-nucleus total elastic cross section at $q^2 = 0$ and $F_{\text{SI}}^2(q^2)$ is the normalized ($F_{\text{SI}}^2(0) = 1$) nonzero-momentum-transfer spin-independent nuclear form-factor. The q^2 -dependence of the SD cross section is governed by the spin-dependent structure function $S_{\text{SD}}^A(q)$ of Engel et al. [1, 39]

$$S_{\text{SD}}^A(q) = S^A(q) = \sum_{L \text{ odd}} (|\langle N || \mathcal{T}_L^{el5}(q) || N \rangle|^2 + |\langle N || \mathcal{L}_L^5(q) || N \rangle|^2). \quad (3)$$

The transverse electric $\mathcal{T}^{el5}(q)$ and longitudinal $\mathcal{L}^5(q)$ multipole projections of the axial vector current operator are given in the Appendix.

Relic WIMPs in the halo of our Galaxy have a mean velocity of $\langle v \rangle \simeq 300 \text{ km/s} = 10^{-3}c$. When $R \ll 1/q_{\text{max}}$ (or $q_{\text{max}}R \ll 1$) where R is the nuclear size and $q_{\text{max}} = 2\mu_A v$ is the maximum of the momentum transfer in the χ -nucleus scattering, the spin structure function $S^A(q)$ reduces to (so-called *zero transfer momentum limit*)

$$S^A(0) = \frac{1}{4\pi} |\langle A || \sum_i \frac{1}{2} (a_0 + a_1 \tau_3^i) \sigma_i || A \rangle|^2 = \frac{2J+1}{\pi} J(J+1) \Lambda^2 \quad \text{with} \quad \Lambda = \frac{a_p \langle \mathbf{S}_p \rangle}{J} + \frac{a_n \langle \mathbf{S}_n \rangle}{J}.$$

Here $\langle \mathbf{S}_{p,n} \rangle$ is the proton (or neutron) spin averaged over nucleus A , a_n and a_p are the effective spin WIMP-neutron and WIMP-proton couplings that contain details of the supersymmetric model, as well as the quark spin content of the proton and neutron.

As m_χ increases, $R \approx 1/q$ (the product qR starts to become non-negligible) and *the finite momentum transfer limit* must be considered for heavier nuclei. The formalism is a straight forward extension of that developed for the study of weak and electromagnetic semi-leptonic interactions in nuclei. Here we follow the definitions of [40, 41]. With the isoscalar spin coupling constant $a_0 = a_n + a_p$ and the isovector spin coupling constant $a_1 = a_p - a_n$ one can split the nuclear structure function $S^A(q)$ into a pure isoscalar term, $S_{00}^A(q)$, a pure isovector term, $S_{11}^A(q)$, and an interference term, $S_{01}^A(q)$, in the following way:

$$S^A(q) = a_0^2 S_{00}^A(q) + a_1^2 S_{11}^A(q) + a_0 a_1 S_{01}^A(q). \quad (4)$$

These three partial structure functions contain expectation values of operators of the form $j_L(qr)[Y_L \sigma]^{L\pm 1}$, which depend on spatial coordinates and nucleon spins. The relations

$$\begin{aligned} S_{00}^A(0) &= C(J) (\langle \mathbf{S}_p \rangle + \langle \mathbf{S}_n \rangle)^2, & S_{11}^A(0) &= C(J) (\langle \mathbf{S}_p \rangle - \langle \mathbf{S}_n \rangle)^2, \\ S_{01}^A(0) &= 2C(J) (\langle \mathbf{S}_p^2 \rangle - \langle \mathbf{S}_n^2 \rangle) & \text{with} \quad C(J) &= \frac{2J+1}{4\pi} \frac{J+1}{J}, \end{aligned} \quad (5)$$

connect the nuclear spin structure function $S^A(q)$ at $q = 0$ with proton $\langle \mathbf{S}_p \rangle$ and neutron $\langle \mathbf{S}_n \rangle$ spin contributions averaged over the nucleus. In relations (5) the normalization coefficient $C(J) > 0$ and therefore $S_{00}(0) \geq 0$ and $S_{11}(0) \geq 0$. These three partial structure functions $S_{ij}^A(q)$ allow calculation of spin-dependent cross sections for any heavy Majorana particle as well as for the neutralino with arbitrary composition [42].

In this paper we extend our consideration of the modern nuclear spin structure calculations involved into the problem of the direct dark matter search. The calculations of the proton and neutron spins $\langle \mathbf{S}_{p(n)} \rangle$ averaged over all nucleons in the nucleus A , which are relevant to the zero-momentum neutralino-nucleon spin cross sections, are considered in our previous review [7]. The cross sections at zero momentum transfer show strong dependence on the nuclear structure of the ground state [28]. Here we discuss the calculations of the spin structure functions in the *finite* momentum transfer approximation. We also touch upon the level of accuracy of these calculations. Finally, (in the last section) we briefly discuss a new approach to data analysis in the finite momentum transfer approximation directly in terms of the effective spin nucleon couplings $a_{0,1}$ together with the scalar WIMP-proton cross section $\sigma_{\text{SI}}^p(0)$ at $q = 0$. Contrary to other possibilities, (see for example, [43]), this procedure is direct and relies as much as possible on the results of the most accurate nuclear spin structure calculations.

II. NON-ZERO MOMENTUM TRANSFER LIMIT

To the best of our knowledge, the finite, non-zero momentum transfer calculations of the spin nuclear structure functions $S^A(q)$ have been performed for the set of isotopes given in Table I. The zero-momentum transfer limit (mostly quenching) is also investigated for Cd, Cs, Ba and La [47, 49, 50], for hydrogen, ^1H , [51, 52], helium, ^3He , [44], chlorine, ^{35}Cl , [40] and calcium, ^{43}Ca , [33].

General discussion of the nuclear model approaches to calculation of the spin characteristics like spins averaged over the nucleus proton (neutron) $\langle \mathbf{S}_{p(n)} \rangle$, one can find in our previous paper [7]. In this paper all available sets of the spin structure functions are given either in the form of explicit functions or as useful analytical parameterizations of the accurate numerical results, or only graphically (as pictures from original papers).

As already noted in the introduction for quite heavy WIMPs and sufficiently heavy nuclei,

TABLE I: List of isotopes with available spin structure functions, $S^A(q)$, at $q > 0$.

| A | Isotope | Authors and reference(s) |
|-----|------------------------------|---|
| 19 | Fluorine, ^{19}F | Vergados et al. [26, 28, 44] |
| 23 | Sodium, ^{23}Na | Ressell and Dean [41] Vergados et al. [28, 41] |
| 27 | Aluminium, ^{27}Al | Engel et al. [42] |
| 29 | Silicon, ^{29}Si | Ressell et al. [40] Vergados et al. [26, 28] |
| 39 | Potassium, ^{39}K | Engel et al. [42] |
| 73 | Germanium, ^{73}Ge | Ressell et al. [40] Demitrov et al. [45] |
| 93 | Niobium, ^{93}Nb | Engel et al. [46] |
| 123 | Tellurium, ^{123}Te | Nikolaev and Klapdor-Kleingrothaus [47] |
| 125 | Tellurium, ^{125}Te | Ressell and Dean [41] |
| 127 | Iodide, ^{127}I | Ressell and Dean [41] |
| 129 | Xenon, ^{129}Xe | Ressell and Dean [41] |
| 131 | Xenon, ^{131}Xe | Engel [1] Ressell and Dean [41] Nikolaev and Klapdor-Kleingrothaus [47] |
| 207 | Lead, ^{207}Pb | Vergados and Kosmos [44, 48] |

the dependence of the nuclear matrix elements on the momentum transfer cannot be ignored even if the WIMP has energies as low as 100 keV. For example, if $m_\chi \gg m_A$, the reduced mass μ_A almost reaches m_A ($\mu_A \rightarrow m_A$). It is rather popular (and simplest) assumption that the WIMPs have a Maxwellian velocity distribution in the halo of our Galaxy. Some WIMPs will possess velocities significantly greater than $\langle v \rangle \simeq 10^{-3}c$. A maximum velocity of $v_{\max} \simeq 700$ km/s (slightly greater than the Galactic escape velocity and more than twice the mean WIMP velocity) implies maximum momentum transfers of $q_{\max} \simeq 550$ MeV for nuclei with atomic weight $A \sim 127$. This q value is not *small* compared to the inverse nuclear size [41] and one has to use *the finite momentum transfer approximation* for heavier nuclei.

Despite the above-mentioned simple kinematic estimation of q_{\max} (which is used over the text for illustration) it is worth noting that this q_{\max} value is in fact too large and is almost not reachable. The WIMP-nucleus interaction is very weak, it occurs very rarely and therefore the impulse approximation for rather large q is well motivated and is used almost in all nuclear calculations reviewed in the paper. In the impulse approximation the WIMP-nuclear interac-

tion is described by means of the WIMP interaction with a nucleon from the nucleus A (see Appendix) and the maximal momentum transfer in the WIMP-nucleon system is considerably smaller than the q_{\max} . Therefore for heavy enough nuclei, in general, the transfer momentum $q \ll q_{\max}$.

The full momentum dependence of the form factors must be calculated from detailed nuclear models, and the results are especially important for heavier nuclei [27]. Unfortunately, the simple phenomenological analysis in the OGM (odd group model) and EOGM (extended OGM) of [53] cannot be extended to the finite momentum transfer case, because the experimental data directly related to the neutralino-nucleus elastic scattering is not available [1]. Quite a number of high multipoles can now contribute, some of them getting contributions from components of the wave function which do not contribute in the static limit (i.e. at $q = 0$). Thus, in general, sophisticated Shell Model calculations are needed to account both for the observed retardation of the static spin matrix element and its correct dependence on transfer momentum, q . For the experimentally interesting nuclear systems $^{29}_{14}\text{Si}$ and $^{73}_{32}\text{Ge}$ very elaborate calculations have been performed by Ressel et al. [40]. In the case of $^{73}_{32}\text{Ge}$ a further improved calculation by Dimitrov, Engel and Pittel was carried out [45] by suitably mixing variationally determined triaxial Slater determinants. Indeed, for this complex nucleus many multipoles contribute and the needed calculations involve techniques which are extremely sophisticated [48]. Now the necessity for more detailed calculations *especially* for the spin-dependent component of the cross sections for heavy nuclei is well motivated.

Further available sets of spin structure functions $S^A(q)$ are collected for nuclei from ^{19}F up to the ^{207}Pb .

A. Fluorine, ^{19}F

Fluorine-19 is the isotope most sensitive to the spin-dependent WIMP-nuclear interaction [28] and a lot of experimental groups hope to explore this feature of ^{19}F experimentally (see, for example, [10, 15, 54, 55, 56, 57]).

The finite momentum transfer spin structure function $S^{19}(q)$ for ^{19}F , one of the lightest DM target medium, (together with other light targets ^{23}Na and ^{29}Si) was obtained for the first time by Vergados with co-authors [28]. The spin contribution to the differential cross section was carefully estimated by the shell-model calculations in the sd shell using the Wildenthal

interaction (see, for example, [58, 59]), which was developed and tested over many years. This interaction is known to reproduce accurately many nuclear observables for *sd* shell nuclei. The Wildenthal two-body matrix elements as well as the single-particle energies are determined by fits to experimental data in nuclei from $A = 17$ to $A = 39$. The shell-model wave functions used by the authors were tested in the calculation of the low-energy spectra and ground state magnetic moment. Rather good agreement between the theoretical and experimental results was achieved (see Tables 2–4 in our previous review [7]). Their spin matrix elements are in good agreement with those of previous calculations [40].

The pure isoscalar, S_{00}^{19} , pure isovector, S_{11}^{19} , and interference, S_{01}^{19} terms (4) of the fluorine ($J = 1/2$) structure function $S^{19}(q)$ can be given in the form [28]:

$$\begin{aligned} S_{00}^{19}(q) &= \frac{2J+1}{16\pi} \times (2.610) \times e^{-u} \{P_{(0,1)}^2(u) + P_{(2,1)}^2(u)\}, \\ S_{11}^{19}(q) &= \frac{2J+1}{16\pi} \times (2.807) \times e^{-u} \{Q_{(0,1)}^2(u) + Q_{(2,1)}^2(u)\}, \\ S_{01}^{19}(q) &= \frac{2J+1}{8\pi} \times (2.707) \times e^{-u} \{P_{(0,1)}(u)Q_{(0,1)}(u) + P_{(2,1)}(u)Q_{(2,1)}(u)\}. \end{aligned} \quad (6)$$

Here the following functions are introduced:

$$\begin{aligned} P_{(0,1)}(u) &= 0.1145u^2 - 0.6667u + 1, & Q_{(0,1)}(u) &= 0.1088u^2 - 0.6667u + 1, \\ P_{(2,1)}(u) &= -0.0026u^2 + 0.0100u, & Q_{(2,1)}(u) &= 0.0006u^2 + 0.0041u. \end{aligned}$$

The dimensionless variable $u = (qb)^2/2$ and the energy transfer to the nucleus A are connected by the relation $E = ub^{-2}/M_A$ (or $u = b^2 E M_A$). Here $b = 1.00A^{1/6} = 1.63 \text{ fm} = 1.63/0.1973 \text{ GeV}^{-1}$ is the oscillator size parameter for ^{19}F . For $v_{\text{max}} \approx 600 \text{ km/s}$ one has $u_{\text{max}} \approx 0.17$ (or $q_{\text{max}} \approx 71 \text{ MeV}$, and $E_{\text{max}} \approx 140 \text{ keV}$) and $u_{\text{min}} \approx 0.011$, which corresponds to the energy threshold of 10 keV (and $q_{\text{min}} \approx 17 \text{ MeV}$).

Following [28] we note that at a relatively large momentum transfer the nucleonic axial current gets modification (PCAC) $\vec{\sigma} \rightarrow \vec{\sigma} - \frac{(\vec{\sigma} \cdot \vec{p})\vec{p}}{q^2 + m_\pi^2}$. Therefore structure functions (6) become more complicated:

$$\begin{aligned} S_{00}^{19}(q) &= \frac{2.610}{8\pi} e^{-u} \{P_{(0,1)}^2(u)(1 + \beta_0(u)) + P_{(2,1)}^2(u)(1 + \beta_2(u)) - 2\beta_{02}(u)P_{(0,1)}(u)P_{(2,1)}(u)\}, \\ S_{11}^{19}(q) &= \frac{2.807}{8\pi} e^{-u} \{Q_{(0,1)}^2(u)(1 + \beta_0(u)) + Q_{(2,1)}^2(u)(1 + \beta_2(u)) - 2\beta_{02}(u)Q_{(0,1)}(u)Q_{(2,1)}(u)\}, \\ S_{01}^{19}(q) &= \frac{2.707}{4\pi} e^{-u} \{P_{(0,1)}(u)Q_{(0,1)}(u)(1 + \beta_0(u)) + P_{(2,1)}(u)Q_{(2,1)}(u)(1 + \beta_2(u)) \\ &\quad - \beta_{02}(u) \times (P_{(0,1)}(u)Q_{(2,1)}(u) + Q_{(0,1)}(u)P_{(2,1)}(u))\}, \end{aligned} \quad (7)$$

where

$$\beta_0(u) = \frac{1}{3} \left[\left(\frac{u_\pi}{u + u_\pi} \right)^2 - 1 \right], \quad \beta_2(u) = 2\beta_0(u), \quad \beta_{02}(u) = -\sqrt{2}\beta_0(u), \quad u_\pi = \frac{(bm_\pi)^2}{2}. \quad (8)$$

When $m_\pi \rightarrow \infty$ formulas, (7) pass into (6). The fluorine structure functions calculated in

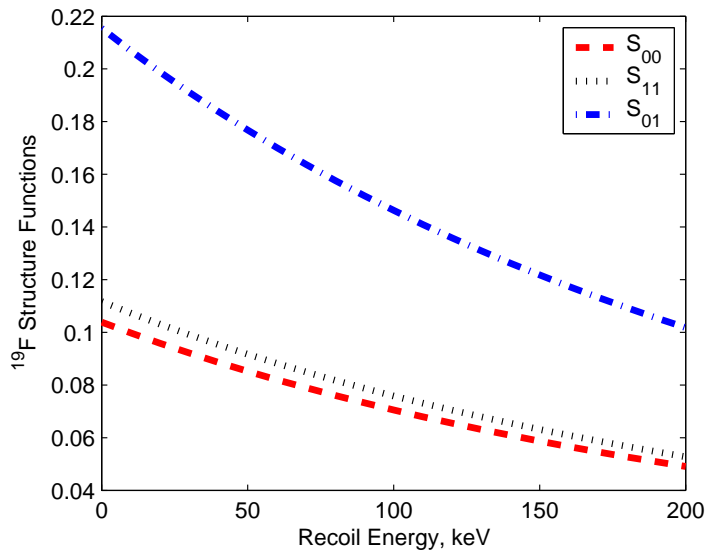


FIG. 1: Structure functions S_{00}^{19} (bottom), S_{11}^{19} (middle), and S_{01}^{19} (top) for ^{18}F as a function of the recoil energy $E = ub^{-2}/M_A$ in keV calculated by (7). With $v_{\max} \approx 600(700)$ km/s for the ^{18}F target one has $E_{\max} \approx 140(190)$ keV.

accordance with (7) are given in Fig. 1 as functions of the recoil energy. Further details can be found in the original paper [28].

B. Sodium, ^{23}Na

In the modern most promising scintillator dark matter detectors (like, for example, the DAMA one) iodine is always used together with sodium in the form of large sodium iodide (NaI) crystals (see for example, [31, 60, 61, 62, 63]). The nucleus ^{23}Na ($J = 3/2$) lies in the middle of the sd shell and therefore the methods applied to other sd -shell nuclei [41] can be used. Ressel and Dean [41] have performed calculation for ^{23}Na exactly analogous to those done for ^{29}Si in [40] and for ^{27}Al in [42], including the use of harmonic oscillator wave functions. The following zero-transfer-limit spin structure parameters are obtained: $\langle \mathbf{S}_p^{23} \rangle = 0.2477$ and $\langle \mathbf{S}_n^{23} \rangle = 0.0198$ [40, 42]. The fits to the structure functions $S_{ij}^{23}(q)$ as third order polynomials in $y = (qb/2)^2$ are given as follows [41]:

$$\begin{aligned} S_{00}^{23}(y) &= 0.0380 - 0.1743 y + 0.3783 y^2 - 0.3430 y^3, \\ S_{01}^{23}(y) &= 0.0647 - 0.3503 y + 0.9100 y^2 - 0.9858 y^3, \\ S_{11}^{23}(y) &= 0.0275 - 0.1696 y + 0.5077 y^2 - 0.6180 y^3. \end{aligned} \quad (9)$$

Here y is obviously well below 1, the functions are rather accurate to $y < y_{\max} = 0.1875$ ($q_{\max} \approx 100$ MeV), which corresponds to the maximum halo velocity of $v_{\max} = 700$ km/s and the heavy enough WIMP mass. Here the oscillator parameter $b = 1.6864$ fm $= (1/117.01)$ MeV $^{-1}$ is used.

Using their shell-model approach Vergados with co-authors also calculated the spin structure function $S^{23}(q)$ for ^{23}Na [28]. Their three terms of the $S^{23}(q)$ ($J = 3/2$) are

$$\begin{aligned} S_{00}^{23}(q) &= \frac{2J+1}{16\pi} \times (0.478) \times e^{-u} \left\{ P_{(0,1)}^2(u) + P_{(2,1)}^2(u) + P_{(2,3)}^2(u) + P_{(4,3)}^2(u) \right\}, \\ S_{11}^{23}(q) &= \frac{2J+1}{16\pi} \times (0.346) \times e^{-u} \left\{ Q_{(0,1)}^2(u) + Q_{(2,1)}^2(u) + Q_{(2,3)}^2(u) + Q_{(4,3)}^2(u) \right\}, \\ S_{01}^{23}(q) &= \frac{2J+1}{8\pi} \times (0.406) \times e^{-u} \left\{ P_{(0,1)}(u)Q_{(0,1)}(u) + P_{(2,1)}(u)Q_{(2,1)}(u) + \right. \\ &\quad \left. + P_{(2,3)}(u)Q_{(2,3)}(u) + P_{(4,3)}(u)Q_{(4,3)}(u) \right\}, \end{aligned} \quad (10)$$

$$\text{where } P_{(0,1)}(u) = 0.0477u^2 - 0.6667u + 1, \quad Q_{(0,1)}(u) = 0.0465u^2 - 0.6667u + 1,$$

$$P_{(2,1)}(u) = -0.0177u^2 + 0.1048u, \quad Q_{(2,1)}(u) = -0.0349u^2 + 0.1494u,$$

$$P_{(2,3)}(u) = -0.0767u^2 + 0.6092u, \quad Q_{(2,3)}(u) = -0.0894u^2 + 0.7405u,$$

$$P_{(4,3)}(u) = 0.0221u^2, \quad Q_{(4,3)}(u) = 0.0287u^2.$$

The dimensionless variable $u = (qb)^2/2 \equiv 2y$, $b = 1.00A^{1/6} = 1.69$ fm is the oscillator size parameter for ^{23}Na . Relevant spin static characteristics of [28] $\langle \mathbf{S}_p^{23} \rangle = 0.2477$ and $\langle \mathbf{S}_n^{23} \rangle = 0.0199$ are almost exactly equal to ones from [41]. In Fig. 2 the recoil energy dependence of the spin structure functions calculated for ^{23}Na by (9) and (10) is presented. One can see from Fig. 2 that the isoscalar spin functions S_{00}^{23} have practically the same behavior in the left and right panels, but, despite the same normalization at $q = 0$, the isovector S_{11}^{23} and mixed S_{01}^{23} spin functions from Vergados et al. [28] (in the right panel) are systematically a bit larger than the S_{11}^{23} and S_{01}^{23} functions from Ressel and Dean [41] (in the left panel of Fig. 2).

C. Aluminum, ^{27}Al

The ^{27}Al nucleus is one of the active ingredients in a very high-resolution and low-threshold sapphire-crystal (Al_2O_3) CRESST detector [64]. Engel, Ressel, Towner, and Ormand in [42] carried out calculations with the Lanczos m-scheme shell-model code CRUNCHER [65]. The m-scheme basis for ^{27}Al contains 80115 Slater determinants. The agreement of the calculated

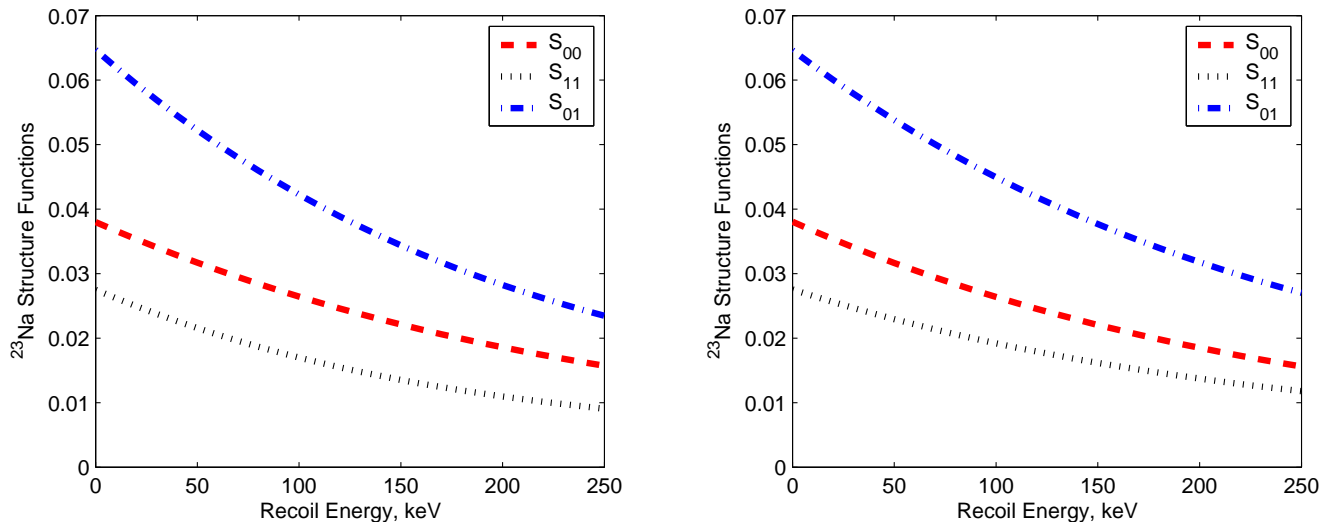


FIG. 2: Spin structure functions for ^{23}Na S_{00}^{23} (middle), S_{11}^{23} (bottom), and S_{01}^{23} (top) versus the recoil energy. Left: S_{ij}^{23} approximations from Ressel and Dean [41] in accordance with (9). Right: S_{ij}^{23} from Vergados et al. [28] following (10). With $v_{\text{max}} \approx 700$ km/s for ^{23}Na target one has $E_{\text{max}} \approx 230$ keV.

spectrum with that measured in ^{27}Al is very good. A similar calculation for ^{29}Si was fulfilled by Ressel et al. [40]. In the shell model, the expectation value of any one-body operator and therefore the structure functions can be easily calculated. To evaluate the $S^{27}(q)$ Engel, Ressel, Towner, and Ormand used a nuclear mean-field potential which is closer to the Woods-Saxon rather than the harmonic oscillator form. The length parameter $b = 1.73$ fm for the oscillator functions and the standard parameters for the Woods-Saxon potential were used [42] in calculation of the structure functions. The most accurate ^{27}Al structure functions of [42]

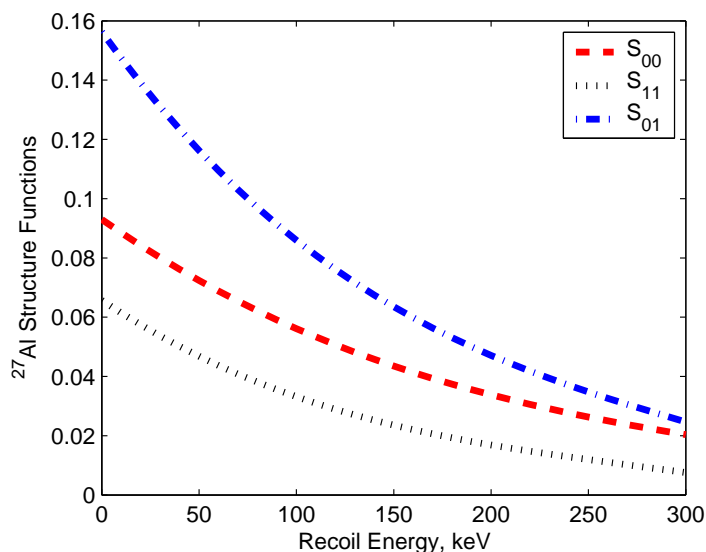


FIG. 3: Structure functions S_{00}^{27} (middle), S_{11}^{27} (bottom), and S_{01}^{27} (top) for ^{27}Al as a function of the recoil energy calculated by (11). For ^{27}Al and the WIMP maximal velocity of 700 km/s the maximum momentum transfer is $q_{\text{max}} \approx 117$ MeV and $E_{\text{max}} \approx 270$ keV.

with the Woods-Saxon single-particle wave functions can be given to a high accuracy by the third-order polynomials

$$\begin{aligned}
 S_{00}^{27}(q) &= 0.0930 - 0.4721 y + 1.0600 y^2 - 1.0115 y^3, \\
 S_{11}^{27}(q) &= 0.0657 - 0.4498 y + 1.3504 y^2 - 1.6851 y^3, \\
 S_{01}^{27}(q) &= 0.1563 - 0.9360 y + 2.4578 y^2 - 2.7262 y^3,
 \end{aligned}
 \tag{11}$$

where $y = (bq/2)^2$. Figure 3 shows these functions S_{ij}^{27} for aluminum versus the recoil energy (see formulas (11)). These three functions allow one to calculate the spin-dependent cross sections for the neutralino interaction with the ^{27}Al target [42].

D. Silicon, ^{29}Si

The first accurate calculation of the q -dependence of the spin structure functions for WIMP scattering off ^{29}Si was carried out by Ressel et al. [40]. With a reasonable two-body interaction Hamiltonian Ressel et al. calculated nuclear wave functions in an appropriate model space. The accuracy of those wave functions was checked by comparison of the calculated excited state energy spectrum, magnetic moments, and spectroscopic factors with the experimental observables. The checked ground state wave functions were used for further calculations of static and more complicated finite momentum nuclear matrix elements involved in DM search calculations. Finite momentum transfer matrix elements and cross sections for the spin-dependent elastic scattering of neutralinos from ^{29}Si and ^{73}Ge [40] were evaluated in that shell-model scheme. Both these isotopes have a great number of configuration mixing and require very large model spaces.

In particular, for evaluation of the wave functions for ^{29}Si the universal sd shell-model interaction of Wildenthal (see, for example, [58, 59]) in a full sd shell-model space was used [40] and calculations were carried out with the Lanczos m -scheme shell-model code CRUNCHER [65]. As in the case of ^{27}Al , [42] the m -scheme basis for ^{29}Si contains 80115 Slater determinants. For static spin matrix elements the following values were obtained: $\langle \mathbf{S}_p^{29} \rangle = -0.002$ and $\langle \mathbf{S}_n^{29} \rangle = 0.13$ (given in Table 4 of [7]).

Figure 4 (left panel) shows the recoil energy dependence of the spin partial structure functions S_{00}^{29} , S_{11}^{29} and S_{01}^{29} for ^{29}Si originally calculated in [40] as a function of $y = (bq/2)^2$ with the

oscillator parameter $b = 1.75$ fm for ^{29}Si . With $v_{\text{max}} = 600(700)$ km/s the maximal momentum transfer is $q_{\text{max}} = 0.108(126)$ GeV, $y_{\text{max}} = 0.23(0.31)$ and $E_{\text{max}} = 213(290)$ keV.

For user's convenience, in their earlier work [40] Ressel et al. obtained rather simple parameterizations of the *full* spin structure function $S^{29}(q)$ (quenching is included)

$$S_{\text{fit}}^{29}(y) = 0.00818 (a_0^2 e^{-4.428y} + 1.06a_1^2 e^{-6.264y} - 2.06a_0a_1 e^{-5.413y}), \quad (12)$$

which provides a highly accurate fit to $S^{29}(y)$ for $y < 0.15$. For $y \geq 0.15$ this parameterization begins seriously underestimate the true value of $S^{29}(y)$ [40]. The lack of validity of (12) at high y (or q) is not a serious problem for WIMP masses up to about $600 \text{ GeV}/c^2$. Anyway, when $a_0 \approx a_1$, parameterization (12) does not reproduce accurately the full result of [40] for all y given in the left panel of Fig. 4.

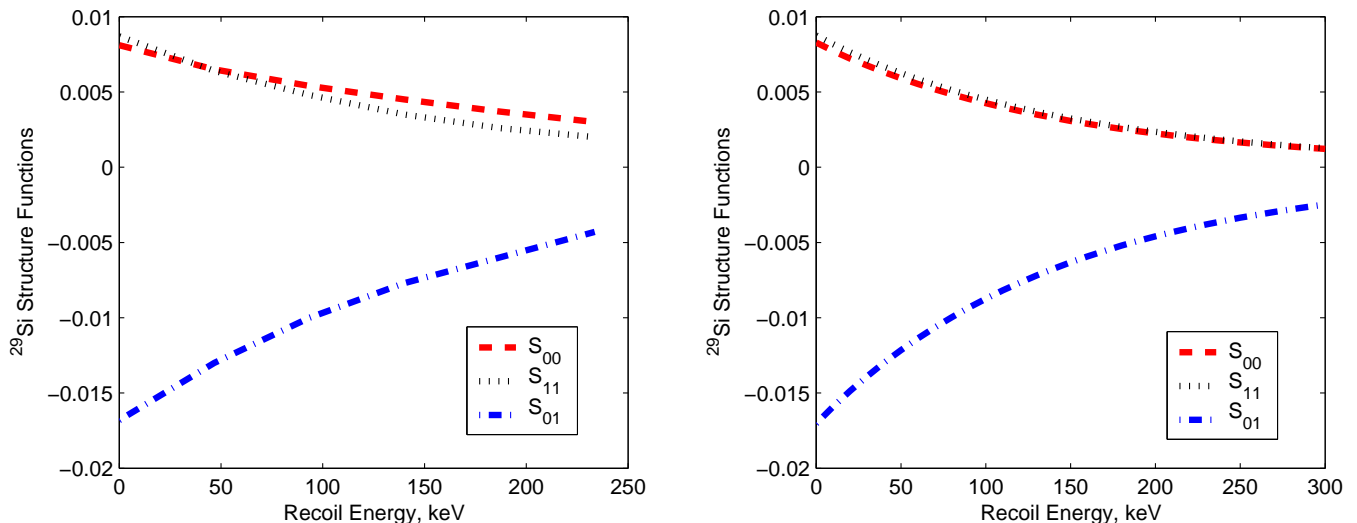


FIG. 4: Spin structure functions S_{00}^{29} (top) S_{11}^{29} (middle), and S_{01}^{29} (bottom) for ^{29}Si as a function of the recoil energy. Left: results of Ressel et al. [40]. Right: these structure functions from Vergados et al. [28] following equations (14). With $v_{\text{max}} \approx 700$ km/s, for ^{29}Si target one has $E_{\text{max}} \approx 290$ keV.

Vergados with co-authors also calculated the spin structure function $S^{29}(q)$ for ^{29}Si in their approach of [28]. The pure isoscalar, S_{00}^{29} , pure isovector, S_{11}^{29} , and interference, S_{01}^{29} terms of the silicon structure function (4) $S^{29}(q)$ ($J^\pi = 1/2^+$) are given in the form

$$\begin{aligned} S_{00}^{29}(q) &= \frac{2J+1}{16\pi} \times (0.208) \times e^{-u} \left\{ P_{(0,1)}^2(u) + P_{(2,1)}^2(u) \right\}, \\ S_{11}^{29}(q) &= \frac{2J+1}{16\pi} \times (0.220) \times e^{-u} \left\{ Q_{(0,1)}^2(u) + Q_{(2,1)}^2(u) \right\}, \\ S_{01}^{29}(q) &= \frac{2J+1}{8\pi} \times (-0.214) \times e^{-u} \left\{ P_{(0,1)}(u)Q_{(0,1)}(u) + P_{(2,1)}(u)Q_{(2,1)}(u) \right\}. \end{aligned} \quad (13)$$

$$\text{where } P_{(0,1)}(u) = 0.2843 u^2 - 0.6667 u + 1, \quad Q_{(0,1)}(u) = 0.2710 u^2 - 0.6667 u + 1,$$

$$P_{(2,1)}(u) = -0.0567 u^2 + 0.4566 u, \quad Q_{(2,1)}(u) = -0.0621 u^2 + 0.4680 u.$$

Here $u = (qb)^2/2 \equiv 2y$. For a rather large momentum transfer, in full analogy with ^{19}F (see, formulas (7)), one has [28]:

$$S_{00}^{29}(q) = \frac{0.208}{8\pi} e^{-u} \left\{ P_{(0,1)}^2(u)(1 + \beta_0(u)) + P_{(2,1)}^2(u)(1 + \beta_2(u)) - 2\beta_{02}(u)P_{(0,1)}(u)P_{(2,1)}(u) \right\},$$

$$S_{11}^{29}(q) = \frac{0.220}{8\pi} e^{-u} \left\{ Q_{(0,1)}^2(u)(1 + \beta_0(u)) + Q_{(2,1)}^2(u)(1 + \beta_2(u)) - 2\beta_{02}(u)Q_{(0,1)}(u)Q_{(2,1)}(u) \right\},$$

$$S_{01}^{29}(q) = \frac{-0.214}{4\pi} e^{-u} \left\{ P_{(0,1)}(u)Q_{(0,1)}(u)(1 + \beta_0(u)) + P_{(2,1)}(u)Q_{(2,1)}(u)(1 + \beta_2(u)) \right. \\ \left. - \beta_{02}(u) (P_{(0,1)}(u)Q_{(2,1)}(u) + Q_{(0,1)}(u)P_{(2,1)}(u)) \right\}, \quad (14)$$

where $\beta_0(u)$, $\beta_2(u)$, and $\beta_{02}(u)$ are defined in (8). Figure 4 (right panel) presents structure functions for ^{29}Si from Vergados et al. [28] following formulas (14). Both sets of spin structure functions for ^{29}Si given in the left [40] and right [28] panels of Fig. 4 are very similar.

E. Potassium, ^{39}K

In the case of ^{39}K the shell-model diagonalization needed for the calculation of the nuclear spin matrix elements requires severe truncations to the active model space. The problem is that ^{39}K is near the boundary between the *sd* and *pf* shells and excitations of particles into higher shells can have significant effects that are often not well simulated by effective operators. Thus, for this nucleus Engel, Ressel, Towner and Ormand [42] used an alternative scheme based on perturbation theory for the evaluation of spin matrix elements. The authors considered two different residual interactions. One is related to the one-boson-exchange potential of the Bonn type, but it is limited only to four or five important meson exchanges. The resulting interaction has a weak tensor-force component typical of Bonn potentials. The other is represented by full G-matrix elements of the Paris potential parameterized in terms of sums over Yukawa functions of various ranges and strengths. This interaction exhibits a strong tensor force. The quality of the wave functions obtained was judged in terms of magnetic moments and Gamow-Teller matrix elements, including meson-exchange currents, isobar currents, and other relativistic effects. The magnetic moments calculated with the help of both interactions differ only slightly from each other and showed good agreement with the corresponding experimental values. The same nuclear wave functions of ^{39}K were also used for the calculation of $\langle \mathbf{S}_p^{39} \rangle$ and $\langle \mathbf{S}_n^{39} \rangle$ and

the structure function $S^{39}(q)$ [42]. Three different sets of spin structure functions for ^{39}K were considered in [42]. They are the “single-particle” functions, the full functions obtained from the modified Bonn interaction, and the full functions obtained from the Paris-based G-matrix.

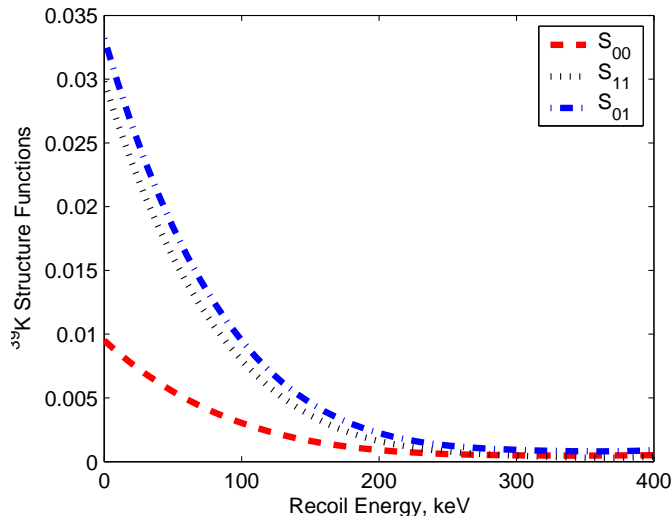


FIG. 5: ^{39}K spin structure functions S_{00}^{39} (top), S_{11}^{39} (middle), and S_{01}^{39} (bottom) versus the recoil energy, calculated by (15) from Engel, Ressel, Towner and Ormand [42]. With $v_{\max} = 700$ km/s, for ^{39}K one has $q_{\max} = 169$ MeV, $E_{\max} = 390$ keV.

There is rather strong reduction of S_{ij}^{39} in comparison with their single-particle values. The strongest reduction is in $S_{00}^{39}(q)$, which is reduced to 25% and 20% of the single-particle value for the two residual interactions. The preferred choice (corresponding to the Paris-based G-matrix approach) can be rather accurately reproduced by the following fourth-order polynomials in $y = (bq/2)^2$ (with $b = 1.84$ fm for ^{39}K):

$$\begin{aligned} S_{00}^{39}(q) &= 0.0095 - 0.0620 y + 0.1628 y^2 - 0.1943 y^3 + 0.0891 y^4, \\ S_{11}^{39}(q) &= 0.0298 - 0.2176 y + 0.6236 y^2 - 0.8144 y^3 + 0.4050 y^4, \\ S_{01}^{39}(q) &= 0.0332 - 0.2319 y + 0.6385 y^2 - 0.7985 y^3 + 0.3810 y^4. \end{aligned} \quad (15)$$

The spin structure functions (15) for ^{39}K are given in Fig. 5. These structure functions allow one to interpret experiments that can look for tracks due to the interaction of dark-matter particles with nuclei in ancient mica [42].

F. Germanium, ^{73}Ge

Germanium isotopes, especially large-spin ($J = 9/2$) ^{73}Ge , are considered to be the most promising material for a real long-running experiment aimed at direct dark matter search. The first experiment with a pure (enriched) ^{73}Ge target was successfully performed at Gran Sasso

by the HDMS collaboration [19, 66]. However, there are fundamental difficulties in describing the spin content of ^{73}Ge due to its complicated collective structure.

The first accurate calculation of the q -dependence of the spin structure functions for WIMP scattering off ^{73}Ge was carried out by Ressel et al. in [40] (together with ^{29}Si). An equally comprehensive calculation was realized by Dimitrov, Engel and Pittel [45]. These authors obtained significantly different (and improved) results in comparison with other studies and they argue that their results are more reliable than the previous ones.

For the study of ^{73}Ge Ressel et al. [40] chose the Petrovich-McManus-Madsen-Atkinson interaction [67], which is a reasonable approximation to a full G-matrix calculation. This interaction proved to be both adequate and tractable in shell model applications. Two different model spaces were considered. The “small” space was determined by an m-scheme basis dimension of 24731 Slater determinants. The “large” space allowed much more excitations with an m-scheme basis dimension of 117137 Slater determinants. Despite fairly large size of the bases, rather severe truncations in the space were implemented. The small space is the smallest one in which it is possible to obtain agreement with the experimental spectrum energy levels. The dimension of the large basis was limited by the computer time and the memory storing constraints [40]. No phenomenological interaction has been developed for Ge-like nuclei and fairly severe truncations to the model space have to be imposed to obtain manageable dimensions. The large model space wave function of ^{73}Ge led to an improved description of the ground state expectation values, in particular of the value of the magnetic moment, in comparison with previous estimates. The calculated magnetic moment μ from [40] exceeds the experimental value, but the authors stressed that the same quenching of both μ and the Gamov-Teller spin matrix elements was almost universally required in shell model calculations of all heavy nuclei. Assuming the isovector spin quenching factor to be 0.833, agreement with the measured μ is obtained. In principle, it is not obvious that quenching is really needed in neutralino- ^{73}Ge scattering but if so, Ressel et al. believed that the correct answer might be in the range between the quenched and unquenched values. It was found (see Table 6 of [7]) that the zero-momentum-transfer spin-neutron matrix element $\langle \mathbf{S}_n^{73} \rangle$ of ^{73}Ge was a factor of 2 larger than the previous predictions. Thus, even if quenching is assumed, the calculated scattering rate is about twice as large as any of the estimates obtained before. Therefore Ressel et al. predicted a higher sensitivity for germanium dark matter detectors [40].

Figure 6 (left panel) shows the recoil energy dependence of the partial structure functions S_{00}^{73} , S_{11}^{73} and S_{01}^{73} for ^{73}Ge calculated by Ressel et al. in [40] in terms of $y = (bq/2)^2$. For ^{73}Ge the oscillator parameter $b = 2.04$ fm, the maximal momentum transfer ($v_{\text{max}} = 600$ km/s) is $q_{\text{max}} = 0.271$ GeV and $E_{\text{max}} = 537$ keV. As in the case of ^{29}Si (see expression (12)) Ressel et al. gave rather simple parameterizations of the *full* spin structure function $S^{73}(q)$ (where quenching is included and which is valid for $y < 0.2$):

$$S_{\text{fit}}^{73}(y) = 0.20313 (1.102a_0^2 e^{-7.468y} + a_1^2 e^{-8.856y} - 2.099a_0a_1 e^{-8.191y}). \quad (16)$$

The lack of validity of (16) for ^{73}Ge at high y (or q) is not a problem for WIMP masses up to about 600 GeV/ c^2 . When $a_0 \approx a_1$, parameterization (16) does not reproduce accurately the full result for all y [40].

A different sophisticated approach to evaluation of the spin structure of ^{73}Ge was considered by Dimitrov, Engel and Pittel in [45]. It relies on the idea of mixing variationally determined Slater determinants, in which symmetries are broken but restored either before or after variation. This approach is described in detail in [68]. In the calculation of [45] the symmetries broken in the intrinsic states are those associated with rotational invariance, parity, and axial shape. The hybrid procedure used restores axial symmetry, parity invariance, and approximate rotational invariance prior to the variation of each intrinsic state. Subsequently, before mixing the intrinsic states the rotational invariance is fully restored. The procedure allows fully triaxial Slater determinants at the expense of particle-number breaking. The results of [68] indicate that the trading of number nonconservation for triaxiality is a good idea, despite the apparent loss of pairing correlations traditionally associated with the former. Pairing forces evidently induce effective triaxiality. The numerical results [68] show that the approach is accurate and efficient for describing even-even systems while also providing reliable reproduction of the collective dynamics of odd-mass systems [45].

For ^{73}Ge the calculations in [45] were performed by assuming, both for protons and neutrons, a single-particle model consisting of the full $0f, 1p$ shell and the $0g_{9/2}$ and $0g_{7/2}$ levels. The main idea was to include all of the single-particle orbits that could play an important role in reproducing low-energy properties of ^{73}Ge [45]. It is well-known that a crucial ingredient in any realistic nuclear-structure calculation is the appropriate form of the nuclear Hamiltonian. The one- and two-body parts of the Hamiltonian have to be compatible with each other as well as with the model space. This is difficult to achieve because microscopic two-body in-

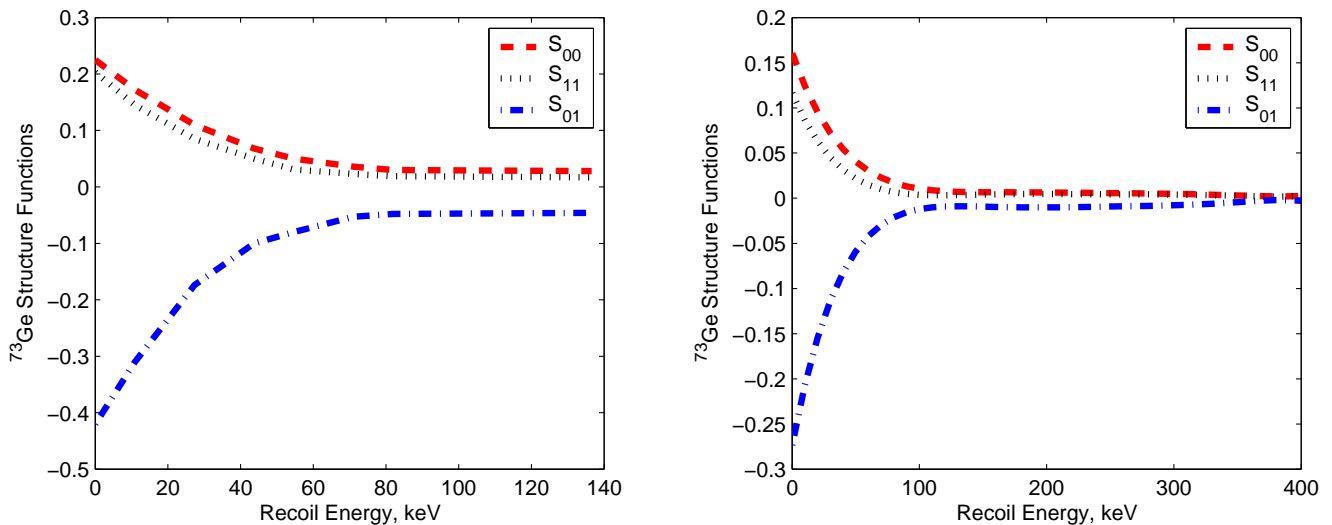


FIG. 6: Spin structure functions S_{00}^{73} (top) S_{11}^{73} (middle), and S_{01}^{73} (bottom) for ^{73}Ge as a function of the recoil energy. Left: results of Ressel et al. [40]. Right: the same structure functions, but from the “hybrid” method of Dimitrov, Engel and Pittel [45] following equations (17). With $v_{\text{max}} \approx 600$ km/s, for the ^{73}Ge target one has $E_{\text{max}} \approx 537$ keV.

teractions, derived for example from a G-matrix, include monopole pieces that are unable to describe the movement of spherical single-particle levels as one passes from the beginning to the end of a shell. A procedure proposed for avoiding this problem consists basically in removing all monopole components from the two-body interaction and shifting their effects to the single-particle energies. This procedure was used by Dimitrov, Engel and Pittel [45] — their two-body force was a fit to the Paris-potential G-matrix modified as described above. The calculated ground-state magnetic dipole moment is in good agreement with the experimental value. Ressel et al. [40] in their large-space shell-model calculation were able to reduce μ significantly to $-1.239\mu_N$ (with experimental value $-0.879\mu_N$) but could not account for the remaining difference. On the contrary, the calculation of Dimitrov, Engel and Pittel, despite the small number of intrinsic states, contains the full quenching required by the experimental data [45]. By making a comparison with the results of Ressel et al. [40], significant disagreement is found for the neutron spin again. The calculated value of Dimitrov, Engel and Pittel is significantly smaller ($-0.920\mu_N$). The differences in the spin contributions, unlike those in the orbital angular momenta, strongly affect the WIMP-Ge scattering cross sections. Thus, contrary to Ressel et al. [40], no significant increase can be expected in the neutralino- ^{73}Ge scattering rate in accordance with [45].

The advantage of Dimitrov, Engel and Pittel's approach to calculation of neutralino cross sections is that it correctly represents the spin structure, requires neither quenching at $q = 0$ nor arbitrary assumptions about the form factor behavior at $q \neq 0$ [45]. Figure 6 (right panel) shows partial structure functions of Dimitrov, Engel and Pittel [45] that determine the spin-dependent cross sections of elastic neutralino scattering off ^{73}Ge .

Comparing the results for $S_{00}^{73}(q)$ (the pure isoscalar form factor) and $S_{11}^{73}(q)$ (the isovector form factor) with the corresponding large-space results of Ressel et al. [40] given in Fig. 6 (left panel) one can conclude that both $S_{00}^{73}(q)$ and $S_{11}^{73}(q)$ of Dimitrov, Engel and Pittel are reduced relative to the curves of Ressel et al. [40].

The polynomial fits, in terms of $y = (bq/2)^2$ with $b = 2.04$ fm being the oscillator parameter for ^{73}Ge , which well represent the structure functions in Fig. 6 (right panel), have the forms of the following sixth-order polynomials [45]:

$$S_{00}^{73}(y) = 0.1606 - 1.1052y + 3.2320y^2 - 4.9245y^3 + 4.1229y^4 - 1.8016y^5 + 0.3211y^6, \quad (17)$$

$$S_{11}^{73}(y) = 0.1164 - 0.9228y + 2.9753y^2 - 4.8709y^3 + 4.3099y^4 - 1.9661y^5 + 0.3624y^6,$$

$$S_{01}^{73}(y) = -0.2736 + 2.0374y - 6.2803y^2 + 9.9426y^3 - 8.5710y^4 + 3.8310y^5 - 0.6948y^6.$$

Here we have to stress that expressions (17) are valid only for $y < 1$ (the smaller y the better the accuracy). At the same time for ^{73}Ge , when the maximal WIMP velocity $v_{\text{max}} = 600$ km/s, one already has the maximal possible momentum transfer $q_{\text{max}} = 0.271$ GeV ($E_{\text{max}} = 537$ keV, $q_{\text{max}}b = 2.08$) and $y_{\text{max}} = 1.96 > 1$. Therefore formulas (17) are obviously *not* valid over the full range of relevant momenta transfer. From Fig. 6 (right panel) it seems, perhaps, rather safe in practice to put all $S_{ij}^{73}(y) = 0$ for $y \geq 1$.

Finally, it will be a very hard task to substantially improve the calculations of Ressel et al. [40] and Dimitrov, Engel and Pittel [45] for these spin matrix elements. Nevertheless, Dimitrov, Engel and Pittel have proposed [45] several possible improvements to their analysis in the future. The most important is an explicit incorporation of the remaining orbits from the $2s, 1d, 0g$ shell, whose effects were treated very roughly in [45]. This should enable one to remove some of the arbitrariness in the single-particle energies that resulted from incomplete treatment of parity-mixing effects, etc (for details see original paper [45]).

G. Niobium, ^{93}Nb

The niobium isotope ^{93}Nb is an odd-group proton nucleus with a large ground-state angular momentum $J = 9/2$. It is a heavy enough nucleus, which can be represented by a basic shell-model space corresponding to three protons in the $1p_{1/2}$ or $0g_{9/2}$ levels and two neutrons in the $1d_{5/2}$ level. This model space was considered by Engel, Pittel, Ormand and Vogel [46]. In order to obtain better agreement with the experiment the authors extended it including in the “large” basis all states in which one proton or one neutron is excited from the above-mentioned “small” space to any level in the sdg -shell. The resulting space contains about 2700 states. They ended up with the nuclear spin matrix elements [46] $\langle \mathbf{S}_p^{93} \rangle = 0.46$ and $\langle \mathbf{S}_n^{93} \rangle = 0.08$ [79].

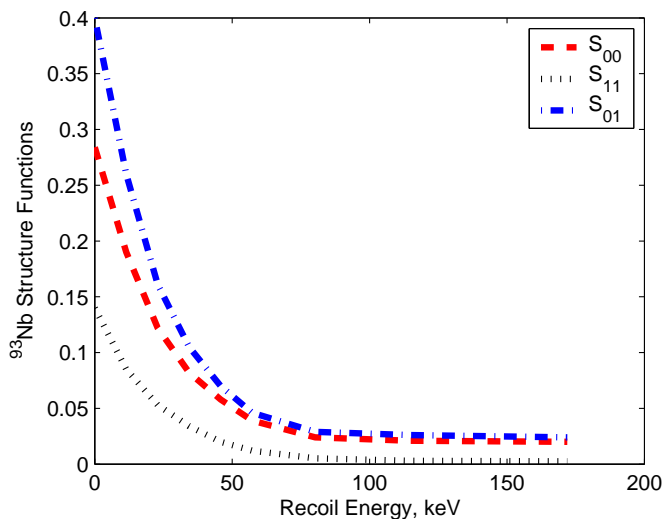


FIG. 7: Partial structure functions $S_{00}^{93}(q)$ (middle), $S_{01}^{93}(q)$ (top) and $S_{11}^{93}(q)$ (bottom) in ^{93}Nb as a function of the recoil energy obtained from paper of Engel, Pittel, Ormand and Vogel [46]. Note that for ^{93}Nb , when the maximal WIMP velocity $v_{\text{max}} = 600$ km/s, one has $q_{\text{max}} = 0.345$ GeV/c (and $q_{\text{max}}^2 = 0.12$ GeV $^2/c^2$), $E_{\text{max}} = 684$ keV and $y_{\text{max}} = 3.48$.

With relation (5) these values can be used to check normalization of the partial spin structure functions $S_{ij}^{93}(q)$ which are available only graphically from Fig. 3 of [46] (and are given here in Table II). In Fig. 7 we present recoil energy dependence of the S_{ij}^{93} structure functions from Table II.

TABLE II: Tabulated partial spin structure functions $S_{ij}^{93}(q)$ from [46] with q^2 in GeV $^2/c^2$.

| q^2 | 0 | 0.002 | 0.004 | 0.006 | 0.008 | 0.01 | 0.014 | 0.02 | 0.03 |
|------------------|-------|-------|-------|-------|-------|-------|--------|-------|--------|
| $S_{01}^{93}(q)$ | 0.4 | 0.26 | 0.161 | 0.105 | 0.07 | 0.046 | 0.029 | 0.026 | 0.024 |
| $S_{00}^{93}(q)$ | 0.284 | 0.19 | 0.122 | 0.082 | 0.058 | 0.039 | 0.024 | 0.021 | 0.02 |
| $S_{11}^{93}(q)$ | 0.14 | 0.085 | 0.053 | 0.034 | 0.02 | 0.012 | 0.0052 | 0.003 | 0.0025 |

An interesting observation concerning interplay between spin-dependent and spin-

independent q -dependencies of nuclear structure functions is given by Engel in [46]. He noted that only nucleons near the Fermi surface contribute significantly to spin-dependent scattering. Because their orbits extend further out than those in the core, the form factor near $q = 0$, which reflects the mean square radius of the contributing nucleons, will always decrease faster for spin-dependent scattering than for spin-independent scattering. By the same token though, the Fermi-surface nucleons have a higher momentum on the average, and the spin-dependent form factors will therefore be larger at high q than their spin-independent counterparts.

On the other hand, for rather light isotopes (F, Na, Si) Vergados et al. [28] claimed the opposite — the drop of the scalar form factor with increasing q is less dramatic compared to that of the spin structure functions. Therefore, contrary to heavy-mass targets, the light-mass targets have a better sensitivity to the scalar interaction for rather large q than to the spin one. Nevertheless, this advantage looks illusive due to the weak A^2 -enhancement of scalar interactions for the low-mass isotopes.

H. Tellurium, $^{123,125}\text{Te}$

The Theory of Finite Fermi Systems was used by Nikolaev and Klapdor-Kleingrothaus [69] to define the q -dependence of nuclear form factors (structure functions) in spin-dependent WIMP scattering off the ^{123}Te isotope. This approach allows one to describe the reduction of single-particle spin-dependent matrix elements in the nuclear medium. Unfortunately, only structure functions for nucleus spin interaction with the *pure bino-like* ($a_0/a_1 = 0.297$) lightest neutralino are presented in [69]. Therefore it is not possible to extract the partial structure functions $S_{ij}^{123}(q)$ for the ^{123}Te isotopes from [69].

Ressell and Dean have performed most accurate nuclear calculations of the neutralino-nucleus spin-dependent cross section for ^{125}Te (together with $^{129,131}\text{Xe}$ and ^{127}I) in [41]. The details of the shell model and residual nucleon-nucleon interactions used in the calculations are given in the next Section. The q -dependence of complete spin structure functions $S_{ij}^{125}(q)$ for ^{125}Te one can be found in Fig. 2 of [41]. Ressel and Dean gave rather simple parameterizations of the complete structure functions $S_{ij}^{125}(q)$ as tables of the coefficients C_k (given in Table III) of 6th order polynomials in y : $S_{ij}^{125}(q) = \sum_{k=0}^6 C_k y^k$, where $y = (qb/2)^2$ and $b = 2.24 \text{ fm} = 11.35/\text{GeV}$ for ^{125}Te . These so-called abbreviated structure functions are only

valid for $y \leq 1$ (or $q = 2\sqrt{y}/b \leq 176$ MeV) and therefore for the recoil energy $E \leq 124$ keV.

TABLE III: ^{125}Te isotope. The first column gives the order of y^k , the next three columns give the corresponding values of the C_k for S_{00}^{125} , S_{01}^{125} , and S_{11}^{125} for the Bonn A calculation. The last three columns present the same results for the Nijmegen II calculation. From [41].

| | Bonn A | | | Nijmegen II | | |
|-------|----------------|----------------|----------------|----------------|----------------|----------------|
| | S_{00}^{125} | S_{01}^{125} | S_{11}^{125} | S_{00}^{125} | S_{01}^{125} | S_{11}^{125} |
| y^0 | 0.0397 | -0.0789 | 0.0392 | 0.0496 | -0.0993 | 0.0496 |
| y^1 | -0.2712 | 0.5727 | -0.3004 | -0.3425 | 0.7315 | -0.3875 |
| y^2 | 0.8694 | -1.9007 | 1.0378 | 1.0666 | -2.3930 | 1.3290 |
| y^3 | -1.5695 | 3.4698 | -1.9460 | -1.8547 | 4.3229 | -2.4952 |
| y^4 | 1.6184 | -3.5546 | 2.0264 | 1.8464 | -4.4282 | 2.6334 |
| y^5 | -0.8797 | 1.9020 | -1.0944 | -0.9762 | 2.3905 | -1.4535 |
| y^6 | 0.1941 | -0.4116 | 0.2380 | 0.2110 | -0.5245 | 0.3241 |

TABLE IV: ^{125}Te isotope. The first column gives the order of y^k , the next three columns give the corresponding values of the C_k for S_{00}^{125} , S_{01}^{125} , and S_{11}^{125} for the Bonn A calculation. The last three columns present the same results for the Nijmegen II calculation. From [41].

| $\times(e^{-2y})$ | Bonn A | | | Nijmegen II | | |
|-------------------|----------------|----------------|----------------|----------------|----------------|----------------|
| | S_{00}^{125} | S_{01}^{125} | S_{11}^{125} | S_{00}^{125} | S_{01}^{125} | S_{11}^{125} |
| y^0 | 0.03971 | -0.07894 | 0.03922 | 0.04960 | -0.09939 | -1.92941 |
| y^1 | -0.19610 | 0.42738 | -0.22938 | -0.24777 | 0.54303 | 1.68075 |
| y^2 | 0.47265 | -1.09331 | 0.62215 | 0.54766 | -1.28816 | -1.16336 |
| y^3 | -0.65023 | 1.55324 | -0.92253 | -0.66553 | 1.67206 | 0.58650 |
| y^4 | 0.54193 | -1.28933 | 0.78465 | 0.47462 | -1.26883 | -0.20730 |
| y^5 | -0.26456 | 0.61844 | -0.38245 | -0.19944 | 0.56728 | 0.05141 |
| y^6 | 0.07489 | -0.16964 | 0.10571 | 0.04819 | -0.14545 | -0.00870 |
| y^7 | -0.01146 | 0.02481 | -0.01542 | -0.00616 | 0.01959 | 0.00087 |
| y^8 | 0.00075 | -0.00152 | 0.00093 | 0.00032 | -0.00107 | 0.00004 |
| $\frac{1}{1+y}$ | 0.0 | 0.0 | 0.0 | 0.0 | 0.0 | 1.97923 |

Ressell and Dean also gave their best parameterization of the complete structure functions $S_{ij}^{125}(q)$ in the form of 8th order polynomials in y multiplied by a factor of $\exp(-2y)$:

$$S_{ij}^{125}(q) = \left(\sum_{k=0}^8 C_k y^k + C_9 \frac{1}{1+y} \right) e^{-2y}. \quad (18)$$

All coefficients C_k for the ^{125}Te isotope are given in Table IV. These so-called *full structure functions* $S_{ij}^{125}(q)$ are valid for all kinetically available $y \leq 10$ (or $q < 557$ MeV) and are presented in Fig. 8 for the Born A potential (three left columns in Table IV).

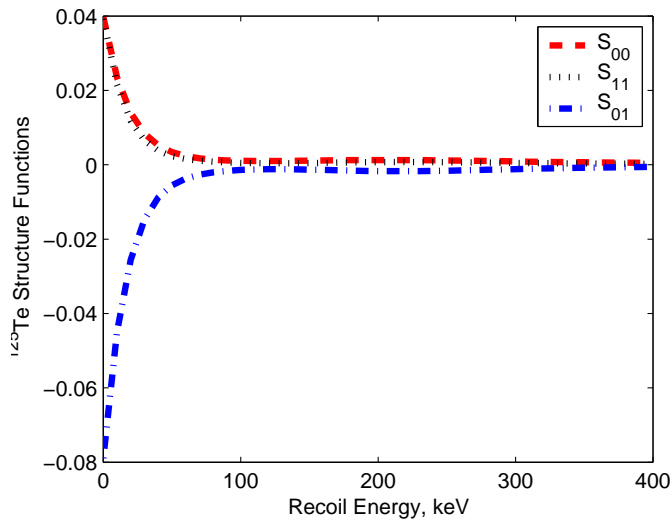


FIG. 8: Partial structure functions $S_{00}^{125}(q)$ (top), $S_{01}^{125}(q)$ (bottom) and $S_{11}^{125}(q)$ (middle) in ^{125}Te as a function of recoil energy obtained from Ressel and Dean [41] by means of parameterization (18). Note that for ^{125}Te , when the maximal WIMP velocity $v_{\text{max}} = 600$ km/s, one has $q_{\text{max}} = 464$ MeV/c, $E_{\text{max}} = 919$ keV and $y_{\text{max}} = 6.95$.

I. Iodine, ^{127}I

The iodine isotope ^{127}I is a decisive component of large sodium iodide (NaI) crystals and therefore plays the most important role in the modern dark matter search (see for example DAMA [31, 60] and ELEGANT, NAIAD and ANAIS experiments [61, 62, 63]).

Ressel and Dean have performed the most accurate nuclear shell-model calculations of the neutralino-nucleus spin-dependent cross section for ^{127}I in [41]. Within the framework of their approach Ressel and Dean considered two residual nuclear interactions based upon recently developed realistic nucleon-nucleon Bonn A [70] and Nijmegen II [71] potentials. These two nucleon-nucleon potentials were used in order to investigate the sensitivity of the results to the particular nuclear Hamiltonian. The Bonn-A-based Hamiltonian was derived for the model space consisting of the $1g_{7/2}$, $2d_{5/2}$, $3s_{1/2}$, $2d_{3/2}$, and $1h_{11/2}$ orbitals, allowing one to include all relevant correlations. In order to get good agreement with observables for nuclei with $A \approx 130$, the single-particle energies (SPEs) were adjusted. The SPEs were varied until reasonable agreement between calculation and experiment was found for the magnetic moment, the low-lying excited state energy spectrum, and the quadrupole moment of ^{127}I . The similar procedure was used by Ressel et al. in [40]. Once the SPEs are specified, a reasonable Hamiltonian can be used for the nuclei under investigation (^{127}I , $^{129,131}\text{Xe}$ and ^{125}Te). The same scheme was used for the Nijmegen II-based Hamiltonian.

To perform a full basis calculation of the ^{127}I ground state properties in the space consisting

of the $1g_{7/2}$, $2d_{5/2}$, $3s_{1/2}$, $2d_{3/2}$, and $1h_{11/2}$ orbitals, one would need basis states consisting of roughly 1.3×10^9 Slater Determinants (SDs). Current calculations can diagonalize matrices with basis dimensions in the range $1-2 \times 10^7$ SDs. Therefore clearly severe truncations of the model space are needed [41]. Fortunately, given the size of the model spaces that can be treated, a truncation scheme that includes the majority of relevant configurations can be devised. Finally (after relevant truncations, see [41] for details) the m-scheme dimension of the ^{127}I model space is about 3 million SDs. The calculated observables agree well with experiment. These interactions do not seem to prefer excitation of more than one extra neutron pair to the $1h_{11/2}$. Most configurations have six neutrons in that orbital, while eight are allowed. Hence, this model space is more than adequate. It is this truncation scheme that was also used for the two xenon isotopes considered ($A = 129$ and 131).

In almost every instance, the results of Ressel and Dean [41] (Tables 8–10 of [7]) show that the spin $\langle \mathbf{S}_i \rangle$ ($i = p, n$) carried by the unpaired nucleon is greater than that found in the other nuclear models. Despite these larger values for $\langle \mathbf{S}_i \rangle$, these calculations have the magnetic moment in good agreement with experiment in all cases. The larger values of $\langle \mathbf{S}_i \rangle$ are due to the fact that more excitations of the even group of the nuclei were allowed [41]. There are visible differences in the response due to the two different forces. In all cases reasonable agreement between calculation and experiment for the magnetic moment (using free particle g -factors) is achieved. It is obvious that the differences between the two calculations are non-trivial but they are quite a bit smaller than the differences coming from the use of alternative nuclear models. This shows that the interaction is not the primary uncertainty in calculations of the neutralino-nucleus spin cross sections [41]. The results obtained by Ressel and Dean give a factor of 20 increase in iodine's sensitivity to spin-dependent scattering over that previously assumed. Due to the form factor suppression the spin response of the sodium iodide detector's is still dominated by ^{23}Na but not to the extent previously thought [41].

The reduced matrix elements of the multipoles in the definition of the $S^A(q)$ (3) are easily evaluated in the harmonic oscillator basis in the nuclear shell model. Almost all calculations of $S^A(q)$ used bases of these harmonic oscillator wave functions. In [41] Ressel and Dean used more realistic Woods-Saxon wave functions to evaluate (3). To check influence of the wave function basis the Bonn A structure function $S^{127}(q)$ for the ^{127}I isotope was also calculated with the harmonic oscillator wave functions. The Woods-Saxon wave functions made a signifi-

cant difference at extremely high momentum transfers when compared to the usual harmonic oscillator wave functions. At more modest momentum transfers the difference is found to be small.

The oscillator parameter, $b = 1 \text{ fm } A^{1/6}$, is usually retained as the size parameter in Woods-Saxon evaluations of $S^A(q)$. In [41] a standard sd -shell parameterization is used: $b = (41.467/\hbar\omega)^{1/2} \text{ fm}$ with $\hbar\omega = 45A^{-1/3} - 25A^{-2/3} \text{ MeV}$. Therefore for all isotopes with $A \approx 127$ one has $b = 2.282 \text{ fm}$. In general, for heavy enough nuclei (say, with $A > 100$) it is especially useful to present structure functions in terms of dimensionless variable $y \equiv (qb/2)^2$. For $y \ll 1$ ($y \geq 1$) the effects of finite momentum transfers are usually rather small (quite large). For these nuclei $y_{\text{max}} = (q_{\text{max}}b/2)^2 \simeq 10 \gg 1$, and nuclear structure form factors are very important. Nevertheless these extremely large values of y are only valid for extremely massive WIMPs ($m_\chi \gg m_A$) moving with an almost escape velocity ($v_{\text{max}} \approx 700 \text{ km/s}$). A more realistic WIMP with mass of about $100 \text{ GeV}/c^2$ moving at an average velocity $v \approx \langle v \rangle = 10^{-3}c$ would have $y_{\text{max}} \simeq 0.4$. Anyway, in order to cover the entire relevant neutralino parameter space, the structure functions were evaluated up to $y = 10$ [41].

The complete partial spin functions $S_{ij}^A(y)$ for ^{127}I , $^{129,131}\text{Xe}$ and ^{125}Te and $y \leq 2$ ($q^2 \simeq 60000 \text{ MeV}^2$), originally calculated by Ressel and Dean with the Bonn-A- and Nijmegen-II-based Hamiltonians, are presented graphically in Fig. 2 of [41]. For practical use Ressel and Dean gave the simple parameterization of ^{127}I structure functions $S_{ij}^{127}(q) = \sum_{k=0}^6 C_k y^k$ as 6th order polynomials in y with C_k coefficients from Table V. These so-called *abbreviated structure functions* are only valid for $y \leq 1$. Ressel and Dean also gave so-called *full structure functions*, which are valid for $y \leq 10$ and reproduce the complete structure functions $S^{127}(q)$ as 8th order polynomials in y multiplied by a factor of $\exp(-2y)$:

$$S_{ij}^{127}(q) = e^{-2y} \sum_{k=0}^8 C_k y^k \quad (19)$$

All coefficients C_k for the ^{127}I isotope are given in Table VI. For example, with the entries in the Bonn A section of Table VI one obtains the analytical forms for ^{127}I spin structure functions:

$$\begin{aligned} S_{00}^{127}(y) &= e^{-2y} \left(0.0983 - 0.4891y + 1.1402y^2 - 1.4717y^3 + 1.1717y^4 \right. \\ &\quad \left. - 0.5646y^5 + 0.1583y^6 - 0.0239y^7 + 0.0015y^8 \right), \\ S_{01}^{127}(y) &= e^{-2y} \left(0.1199 - 0.6184y + 1.5089y^2 - 2.0737y^3 + 1.7731y^4 \right) \end{aligned} \quad (20)$$

$$S_{11}^{127}(y) = e^{-2y} \left(0.0366 - 0.1950y + 0.5049y^2 - 0.7475y^3 + 0.7043y^4 - 0.9036y^5 + 0.2600y^6 - 0.0387y^7 + 0.0024y^8 \right),$$

$$-0.3930y^5 + 0.1219y^6 - 0.0192y^7 + 0.0012y^8).$$

TABLE V: ^{127}I isotope. The first column gives the order of y^k , the next three columns give the corresponding values of the C_k for S_{00}^{127} , S_{01}^{127} , and S_{11}^{127} for the Bonn A calculation. The last three columns present the same results for the Nijmegen II calculation. From [41].

| | Bonn A | | | Nijmegen II | | |
|-------|----------------|----------------|----------------|----------------|----------------|----------------|
| | S_{00}^{127} | S_{01}^{127} | S_{11}^{127} | S_{00}^{127} | S_{01}^{127} | S_{11}^{127} |
| y^0 | 0.0983 | 0.1199 | 0.0365 | 0.1165 | 0.1619 | 0.0562 |
| y^1 | -0.6750 | -0.8436 | -0.2627 | -0.7923 | -1.1403 | -0.4085 |
| y^2 | 2.1353 | 2.7354 | 0.8751 | 2.4985 | 3.7144 | 1.3778 |
| y^3 | -3.7595 | -4.9303 | -1.6146 | -4.3831 | -6.7158 | -2.5702 |
| y^4 | 3.7774 | 5.0581 | 1.6908 | 4.3850 | 6.8938 | 2.7087 |
| y^5 | -2.0091 | -2.7361 | -0.9302 | -2.3222 | -3.7259 | -1.4945 |
| y^6 | 0.4355 | 0.6008 | 0.2069 | 0.5015 | 0.8171 | 0.3329 |

TABLE VI: ^{127}I isotope. The first column gives the order of y^k , the next three columns give the corresponding values of the C_k for S_{00}^{127} , S_{01}^{127} , and S_{11}^{127} for the Bonn A calculation. The last three columns present the same results for the Nijmegen II calculation. From [41].

| $\times(e^{-2y})$ | Bonn A | | | Nijmegen II | | |
|-------------------|----------------|----------------|----------------|----------------|----------------|----------------|
| | S_{00}^{127} | S_{01}^{127} | S_{11}^{127} | S_{00}^{127} | S_{01}^{127} | S_{11}^{127} |
| y^0 | 0.0983 | 0.1199 | 0.0366 | 0.1166 | 0.1621 | 0.0563 |
| y^1 | -0.4891 | -0.6184 | -0.1950 | -0.5721 | -0.8363 | -0.3038 |
| y^2 | 1.1402 | 1.5089 | 0.5049 | 1.3380 | 2.0594 | 0.7948 |
| y^3 | -1.4717 | -2.0737 | -0.7475 | -1.7252 | -2.8319 | -1.1703 |
| y^4 | 1.1717 | 1.7731 | 0.7043 | 1.3774 | 2.3973 | 1.0637 |
| y^5 | -0.5646 | -0.9036 | -0.3930 | -0.6700 | -1.2121 | -0.5713 |
| y^6 | 0.1583 | 0.2600 | 0.1219 | 0.1905 | 0.3486 | 0.1722 |
| y^7 | -0.0239 | -0.0387 | -0.0192 | -0.0292 | -0.0522 | -0.0266 |
| y^8 | 0.0015 | 0.0024 | 0.0012 | 0.0019 | 0.0032 | 0.0017 |

The structure functions $S_{ij}^{127}(y)$ for the ^{127}I isotope and for both nucleon-nucleon forces (Bonn A and Nijmegen II) up to $y = 10$ were carefully analyzed in [41]. Some similarities and differences between these two sets of iodine structure functions were observed. Despite that the differences between the two calculations are non-trivial but they are quite smaller than the differences coming from the use of alternative nuclear models. This shows, in particular,

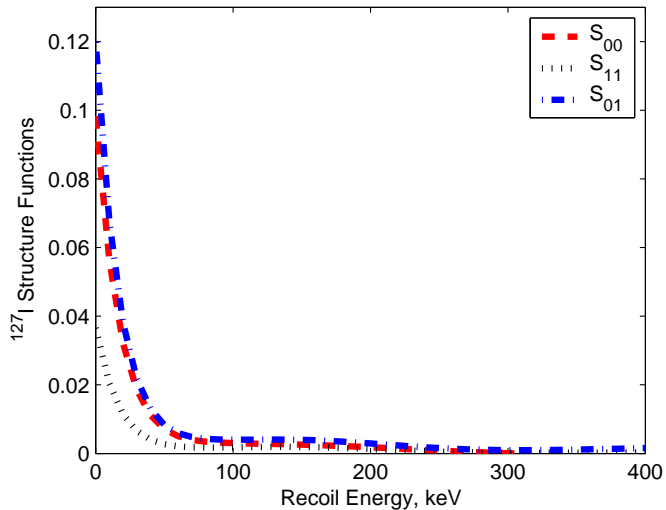


FIG. 9: Partial structure functions of Ressel and Dean S_{ij}^{127} for ^{127}I as a function of recoil energy calculated from formulas (20). Note, for ^{127}I , when the maximal WIMP velocity $v_{\text{max}} = 600$ km/s, one has $q_{\text{max}} \approx 472$ MeV/c, $E_{\text{max}} \approx 934$ keV and $y_{\text{max}} \approx 7.44$.

that the interaction is not the primary uncertainty in calculations of the neutralino-nucleus scattering cross sections [41].

Finally, it is perhaps a right place to note that for $y \approx y_{\text{max}} \approx 7.5$, which already corresponds to a rather large energy ($E_{\text{max}} \approx 900$ keV) transmitted to the target nucleus, one may also expect a non-negligible contribution from *inelastic* WIMP-nuclear interactions not considered here.

J. Xenon, ^{131}Xe and ^{129}Xe

Xenon (gaseous and liquid) is a very popular target material for modern large-scale dark matter detectors (see, for example, [72, 73, 74]). For the first time spin-dependent scattering of SUSY-like dark matter particles from ^{131}Xe ($J = 3/2$) nuclei at non-zero momentum transfer was considered by Engel in [1]. The configuration-mixing quasiparticle Tamm-Dancoff approximation (QTDA) was used. In the zeroth order the ground state of ^{131}Xe was represented as the $1d_{3/2}$ quasineutron excitation of the even-even core $|0\rangle$ treated in the BCS approximation (BCS-based model of the Fermi surface). In order to incorporate nuclear structure corrections originating from the residual interaction three-quasiparticle configurations of the form $[\nu_{d3/2}^\dagger [\nu_k^\dagger \nu_l^\dagger]^K]^{3/2} |0\rangle$ and $[\nu_{d3/2}^\dagger [\pi_k^\dagger \pi_l^\dagger]^K]^{3/2} |0\rangle$ were admixed. Here π^\dagger and ν^\dagger represent the proton and neutron quasiparticle creation operators, K is an arbitrary intermediate angular momentum, and k, l run over a valence space consisting of the $2s$, $1d$, $0g$ and $0h$ harmonic oscillator levels [1]. Despite the fact that the amplitudes associated with the admixed three-quasiparticle

states are small (less than 5%), these admixtures can lead to a substantial effect. The experimental value of the magnetic moment of ^{131}Xe , which is about $0.69\mu_N$, was reproduced with an accuracy of 2%. The same approximation scheme results in $\langle \mathbf{S}_p^{131} \rangle = -0.041$ and $\langle \mathbf{S}_n^{131} \rangle = -0.236$. Figure 10 (left panel) shows Engel's partial structure functions S_{ij}^{131} in ^{131}Xe as a function of the recoil energy, recalculated from Table VII.

TABLE VII: Tabulated spin structure functions $S_{ij}^{131}(q)$ from Fig. 3 of [1].

| q^2 | 0 | 0.0025 | 0.005 | 0.01 | 0.015 | 0.02 | 0.025 | 0.03 | 0.04 | 0.05 | 0.06 |
|-------------------|--------|--------|--------|--------|-------|--------|--------|--------|--------|--------|--------|
| $S_{00}^{131}(q)$ | 0.4 | 0.0215 | 0.014 | 0.01 | 0.009 | 0.008 | 0.0075 | 0.0066 | 0.005 | 0.0035 | 0.0017 |
| $S_{11}^{131}(q)$ | 0.020 | 0.009 | 0.006 | 0.004 | 0.003 | 0.0027 | 0.0025 | 0.0023 | 0.0019 | 0.0015 | 0.001 |
| $S_{01}^{131}(q)$ | -0.056 | -0.028 | -0.019 | -0.013 | -0.01 | -0.009 | -0.008 | -0.007 | -0.005 | -0.003 | -0.001 |

Engel noted again that the spin-dependent cross section in ^{131}Xe falls as the momentum transfer increases, but *more slowly* than the spin-independent cross section. The spin-dependent efficiency is higher than the spin-independent one, being substantially higher for very heavy neutralinos. The relatively long tail of the spin-dependent structure functions is caused by nucleons near the Fermi surface, which do the bulk of the scattering. The core nucleons, which dominate the spin-independent cross section, contribute much less at large q . These are very general statements that should apply to other heavy nuclei as well [1].

The Theory of Finite Fermi Systems (TFFS) was also used by Nikolaev and Klapdor-Kleingrothaus [69] to define the q -dependence of nuclear structure functions (form factors) in spin-dependent WIMP scattering off the ^{131}Xe isotope (as well as ^{123}Te). The quenching effect (at zero and relatively low q), due to reduction of single-particle spin-dependent matrix elements in the nuclear medium, and its disappearance at higher q was observed in [69]. The same q -behavior was also discussed before by Engel et al. [1, 46]. Nevertheless the shape of the $S^{131}(q)$ from [69] differs a bit (at intermediate q) from the one obtained with the oscillator basis in [1]. Unfortunately, partial structure functions $S_{ij}^{131}(q)$ for ^{131}Xe are not available from [69].

The most sophisticated shell-model treatment of the spin structure functions in ^{131}Xe and ^{129}Xe (as well as in ^{127}I and ^{125}Te isotopes) was performed by Ressel and Dean in [41]. The details of the calculations are given in the previous Section. Their complete sets of the structure functions $S^{129,131}(q)$ are valid for all relevant values of the momentum transfer (see Fig. 3 in [41]). Ressel and Dean gave the simple parameterizations of the complete structure functions

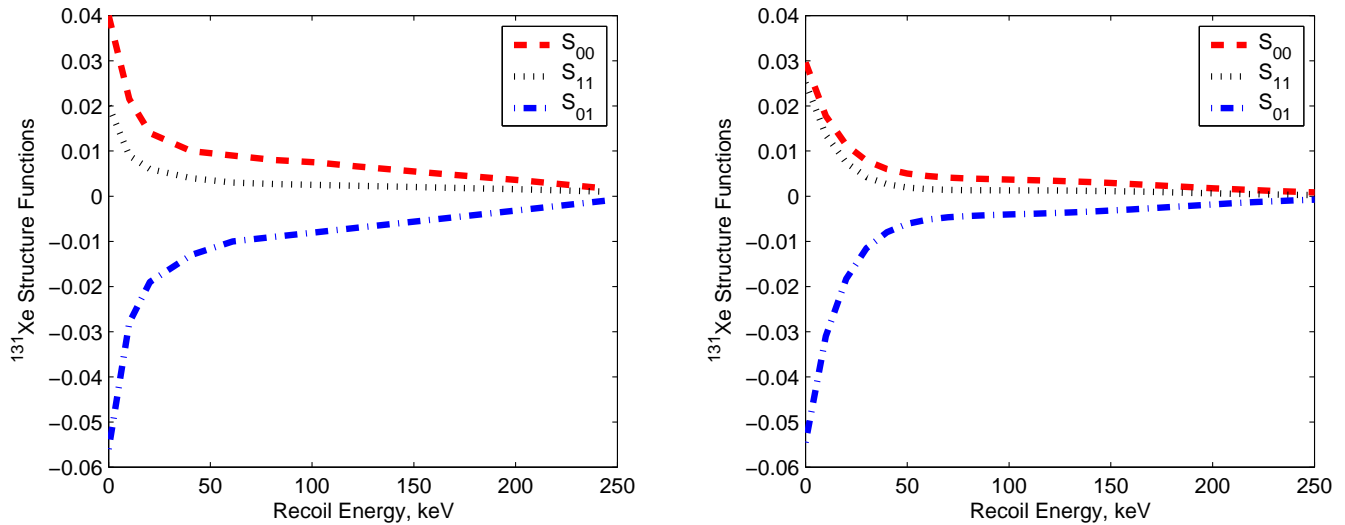


FIG. 10: Partial structure functions $S_{00}^{131}(q)$ (top), $S_{01}^{131}(q)$ (bottom) and $S_{11}^{131}(q)$ (middle) in ^{131}Xe as a function of the recoil energy. Left: results of [1] from Table VII. Right: the full parameterizations of [41] for the Bonn A potential (three left columns in Table IX). Note, that for ^{131}Xe , when the maximal WIMP velocity $v_{\text{max}} = 600$ km/s, one has $q_{\text{max}} \approx 487$ MeV/c, $E_{\text{max}} \approx 963$ keV and $y_{\text{max}} \approx 7.92$.

TABLE VIII: $^{129,131}\text{Xe}$ isotopes. The first column gives the order of y^k , the next three columns give the corresponding values of the C_k for $S_{00}^{129,131}$, $S_{01}^{129,131}$, and $S_{11}^{129,131}$ for the Bonn A calculation. The last three columns present the same results for the Nijmegen II calculation. From [41].

| | Bonn A | | | Nijmegen II | | |
|-------|----------------|----------------|----------------|----------------|----------------|----------------|
| | S_{00}^{129} | S_{01}^{129} | S_{11}^{129} | S_{00}^{129} | S_{01}^{129} | S_{11}^{129} |
| y^0 | 0.0713 | -0.1216 | 0.0518 | 0.0465 | -0.0853 | 0.0392 |
| y^1 | -0.4804 | 0.8745 | -0.3949 | -0.3138 | 0.6150 | -0.2991 |
| y^2 | 1.4726 | -2.8317 | 1.3433 | 0.9656 | -1.9847 | 1.0087 |
| y^3 | -2.5323 | 5.0922 | -2.5152 | -1.6666 | 3.5496 | -1.8648 |
| y^4 | 2.4968 | -5.1976 | 2.6480 | 1.6477 | -3.6023 | 1.9399 |
| y^5 | -1.3071 | 2.7924 | -1.4557 | -0.8642 | 1.9257 | -1.0564 |
| y^6 | 0.2796 | -0.6088 | 0.3228 | 0.1851 | -0.4182 | 0.2326 |
| | S_{00}^{131} | S_{01}^{131} | S_{11}^{131} | S_{00}^{131} | S_{01}^{131} | S_{11}^{131} |
| y^0 | 0.0296 | -0.0545 | 0.0251 | 0.0277 | -0.0497 | 0.0223 |
| y^1 | -0.1852 | 0.3676 | -0.1812 | -0.1754 | 0.3389 | -0.1627 |
| y^2 | 0.5934 | -1.1813 | 0.5932 | 0.5604 | -1.1002 | 0.5427 |
| y^3 | -1.0351 | 2.0529 | -1.0389 | -0.9969 | 1.9709 | -0.9892 |
| y^4 | 1.0049 | -1.9827 | 1.0071 | 1.0100 | -1.9996 | 1.0150 |
| y^5 | -0.5078 | 0.9967 | -0.5071 | -0.5402 | 1.0681 | -0.5459 |
| y^6 | 0.1037 | -0.2026 | 0.1031 | 0.1174 | -0.2316 | 0.1189 |

$S^{129,131}(q)$ as 6th order polynomials in y with coefficients C_k in Table VIII: $S_{ij}^A(q) = \sum_{k=0}^6 C_k y^k$.

These so-called *abbreviated structure functions* are only valid for $y \leq 1$.

For the $^{129,131}\text{Xe}$ isotopes (as previously for ^{127}I and ^{125}Te) Ressel and Dean also presented their parameterization of the *full structure functions* in the following analytical form

$$S_{ij}^A(q) = \left(\sum_{k=0}^8 C_k y^k + C_9 \frac{1}{1+y} \right) e^{-2y}. \quad (21)$$

The form is also valid for $y \leq 10$. The relevant coefficients C_k are given in Table IX. Figure 10

TABLE IX: $^{129,131}\text{Xe}$ isotope. The first column gives the order of y^k , the next three columns give the corresponding values of the C_k for $S_{00}^{129,131}$, $S_{01}^{129,131}$, and $S_{11}^{129,131}$ for the Bonn A calculation. The last three columns present the same results for the Nijmegen II calculation. From [41].

| | Bonn A | | | Nijmegen II | | |
|------------------|----------------|----------------|----------------|----------------|----------------|----------------|
| $\times e^{-2y}$ | S_{00}^{129} | S_{01}^{129} | S_{11}^{129} | S_{00}^{129} | S_{01}^{129} | S_{11}^{129} |
| y^0 | 0.07132 | -0.12166 | -2.05825 | 0.04649 | -0.08538 | -1.28214 |
| y^1 | -0.34478 | 0.64435 | 1.80756 | -0.22551 | 0.45343 | 1.09276 |
| y^2 | 0.75590 | -1.52732 | -1.27746 | 0.49905 | -1.06546 | -0.71295 |
| y^3 | -0.93345 | 2.02061 | 0.65459 | -0.62244 | 1.38670 | 0.31489 |
| y^4 | 0.69006 | -1.57689 | -0.22197 | 0.46361 | -1.05940 | -0.08351 |
| y^5 | -0.30248 | 0.72398 | 0.04546 | -0.20375 | 0.47576 | 0.01059 |
| y^6 | 0.07653 | -0.19040 | -0.00427 | 0.05109 | -0.12208 | 0.00023 |
| y^7 | -0.01032 | 0.02638 | -0.00014 | -0.00671 | 0.01643 | -0.00024 |
| y^8 | 0.00057 | -0.00149 | 0.00004 | 0.00036 | -0.00089 | 0.00002 |
| $\frac{1}{1+y}$ | 0.0 | 0.0 | 2.11016 | 0.0 | 0.0 | 1.32136 |
| $\times e^{-2y}$ | S_{00}^{131} | S_{01}^{131} | S_{11}^{131} | S_{00}^{131} | S_{01}^{131} | S_{11}^{131} |
| y^0 | 0.02964 | -0.05455 | 0.02510 | 0.02773 | -0.04978 | 0.02234 |
| y^1 | -0.13343 | 0.27176 | -0.13772 | -0.12449 | 0.24725 | -0.12206 |
| y^2 | 0.37799 | -0.72302 | 0.36661 | 0.32829 | -0.63231 | 0.31949 |
| y^3 | -0.57961 | 1.05450 | -0.53851 | -0.48140 | 0.89642 | -0.46695 |
| y^4 | 0.57890 | -0.97133 | 0.49255 | 0.47565 | -0.81645 | 0.42877 |
| y^5 | -0.34556 | 0.53842 | -0.26990 | -0.28518 | 0.45235 | -0.23679 |
| y^6 | 0.11595 | -0.16899 | 0.08369 | 0.09682 | -0.14267 | 0.07408 |
| y^7 | -0.02012 | 0.02742 | -0.01340 | -0.01710 | 0.02335 | -0.01197 |
| y^8 | 0.00142 | -0.00181 | 0.00087 | 0.00124 | -0.00156 | 0.00079 |

(right panel) presents parameterizations S_{ij}^{131} from (21) for the Bonn A potential (three left columns in Table IX) as a function of the recoil energy. From Fig. 11, where parameterizations of the full structure functions S_{ij}^{129} are depicted (see Table IX for ^{129}Xe), one can make a general

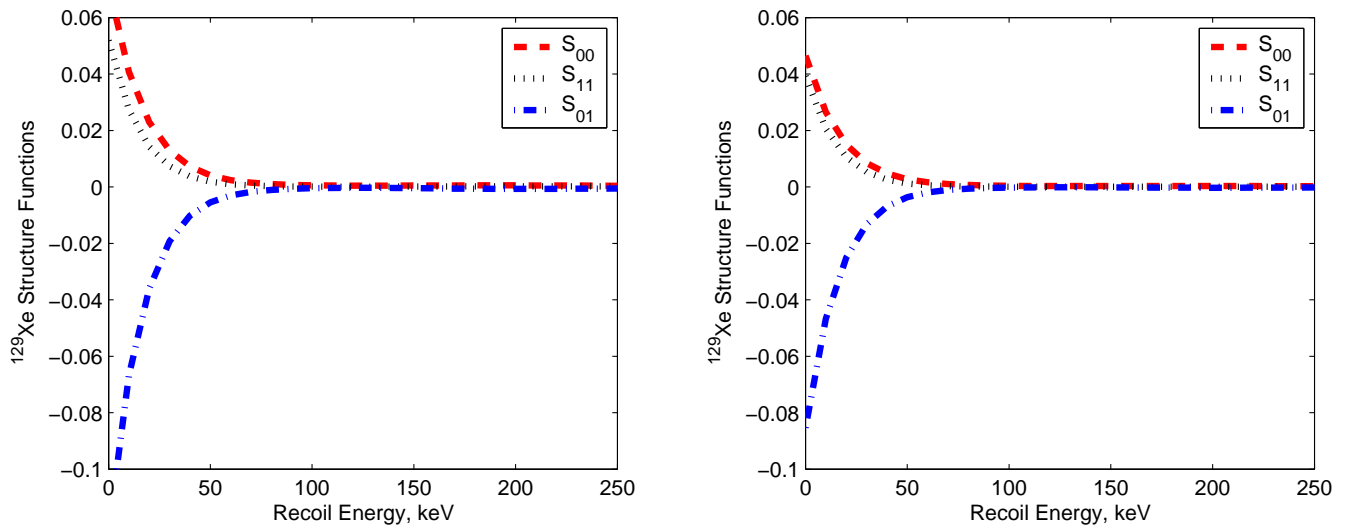


FIG. 11: Partial structure functions $S_{00}^{129}(q)$ (top), $S_{01}^{129}(q)$ (bottom) and $S_{11}^{129}(q)$ (middle) in ^{129}Xe from [41] as a function of the recoil energy. Left: the full parameterizations for the Bonn A potential (three left columns in Table IX). Right: the full parameterizations for the Nijmegen II potential (three right columns in Table IX).

conclusion that there is no large difference between the calculations performed in [41] with the Bonn-A-based and Nijmegen-II-based Hamiltonians.

Structure functions $S^{131}(q)$ for ^{131}Xe have been calculated in the context of two other nuclear models mentioned above, the QTDA by Engel [1] and the TFFS by Nikolaev and Klapdor-Kleingrothaus [69]. Following Ressel and Dean [41], we briefly touch upon the differences in $S^{131}(q)$ that are the result of using different nuclear models. All three calculations show significant quenching compared to the single-particle estimate. The spin distributions obtained in the QTDA and TFFS are somewhat different (see Table 10 from [7]) while the full structure functions (for bino neutralinos) are quite similar. While the values for $\langle \mathbf{S}_n \rangle$ differ very little between Ressel and Dean's and Engel's result in the QTDA, the difference in the values of $S^{131}(0)$ is almost a factor of 2 between the two calculations. It should be noted as well that both the QTDA and the TFFS calculations of $S^{131}(q)$ asymptotically reach the single-particle structure function. This is not the case in Ressel and Dean's calculations, which are well below the single-particle estimate for all values of q^2 . It is apparent that the shell-model-derived structure functions have a much steeper fall-off as a function of q^2 [41]. This difference can be considered as an estimate of the uncertainty followed from the choice of the nuclear model.

Finally, we note that Ressel and Dean in [41] gave accurate structure function parameterizations for the $^{129,131}\text{Xe}$, ^{127}I and ^{125}Te isotopes which are very useful in rather precise calculations of the event rates in heavy-target dark matter detectors. The calculations of Ressel and Dean contain more excitations within the model space and use more modern and realistic nuclear interactions than others in the literature, with a possible exception of the QTDA calculations [1] for ^{131}Xe [41].

K. Lead, ^{207}Pb

Among the nuclei which can be considered as targets for direct dark matter detection, ^{207}Pb seems a potentially rather interesting candidate. The spin matrix element of this nucleus has not been evaluated quite accurately since one expected that WIMP-nuclear spin interaction is important only with light nuclei. But the spin matrix element in the light systems is quenched. On the other hand, the spin matrix element of ^{207}Pb ($J = 1/2$), especially the isoscalar one, does not suffer unusually large quenching, as is known from the study of the magnetic moment [48]. It is believed that ^{207}Pb has a quite simple structure, its ground state can be described as a $2p_{1/2}$ neutron hole outside the doubly magic (closed-shell) nucleus ^{208}Pb . Due to its low angular momentum, only two multipoles $L = 0$ and $L = 2$ can contribute even at large momentum transfers. This is why Kosmas and Vergados in [48] chose ^{207}Pb for investigation of momentum transfer dependence of spin matrix elements in the heaviest possible nuclei relevant to dark matter search. In the $q = 0$ limit Vergados and Kosmas gave the spin matrix element in the simple form $|\mathbf{J}|^2 = |f_A^0 \Omega_0(0) + f_A^1 \Omega_1(0)|^2$, and found that $\Omega_0(0) = -0.95659/\sqrt{3}$ and $\Omega_1(0) = 0.83296/\sqrt{3}$ [44, 48]. The momentum transfer dependence of the total cross section for elastic scattering of cold dark matter candidates, i.e. the lightest supersymmetric particle (LSP), from ^{207}Pb was examined by Kosmas and Vergados in [48, 75, 76, 77].

If the spin-dependent differential cross section is taken in the form of Engel, Ressel et al. [1, 40, 41] and the spin structure function $h(q)$ has the form of Vergados et al. [28]:

$$d\sigma = \frac{8G_{\text{F}}^2}{2J+1} h(q) dq^2, \quad h(q) = \frac{1}{4} \left[(f_A^0)^2 S_{00}^{207}(q) + (f_A^1)^2 S_{11}^{207}(q) + f_A^0 f_A^1 S_{01}^{207}(q) \right],$$

then the partial structure functions for ^{207}Pb $S_{00}^{207}(q)$, $S_{11}^{207}(q)$, and $S_{01}^{207}(q)$ have the form [28]

$$S_{00}^{207}(q) = \frac{2J+1}{16\pi} (0.305) I_{00}(q),$$

$$\begin{aligned}
S_{11}^{207}(q) &= \frac{2J+1}{16\pi} (0.231) I_{11}(q), \\
S_{01}^{207}(q) &= \frac{2J+1}{8\pi} (-0.266) I_{01}(q).
\end{aligned} \tag{22}$$

The spin-dependent neutralino-nucleon couplings $f_A^{0,1}$ are analogous to the parameters $a_{0,1}$ from (4). Finite momentum dependence of these structure functions is concentrated in $I_{ij}(q)$, which can be defined, following [28, 48], as an integral over the forward scattering angle $\xi = \hat{\mathbf{p}}_i \cdot \hat{\mathbf{q}} \geq 0$

$$I_{ij}(q) = 2 \int_0^1 \xi d\xi \frac{\Omega_i(q^2 \xi^2)}{\Omega_i(0)} \frac{\Omega_j(q^2 \xi^2)}{\Omega_j(0)} \tag{23}$$

with $\Omega_i(\mathbf{q}) = (2J+1)^{-1/2} \langle J || \sum_{j=1}^A \sigma(j) \omega_i(j) e^{-i\mathbf{q} \cdot \mathbf{x}_j} || J \rangle$ and $\omega_0(j) = 1$, $\omega_1(j) = \tau_3(j)$.

Here $\sigma(j)$, $\tau_3(j)$, \mathbf{x}_j are the spin, the third component of the isospin ($\tau_3|p\rangle = |p\rangle$), and the coordinate of the j th nucleon, \mathbf{q} is the momentum transferred to the nucleus.

To a good approximation, the ground state of the $^{207}_{82}\text{Pb}$ nucleus can be described as a $2p_{1/2}$ neutron hole in the $^{208}_{82}\text{Pb}$ closed shell [48]. Then for the $L = 0$ multipole one finds

$$\Omega_1(\mathbf{q}) = (1/\sqrt{3})F_{2p}(\mathbf{q}^2) = -\Omega_0(\mathbf{q}) \quad \text{and} \quad I_{00} = I_{01} = I_{11} = 2 \int_0^1 \xi [F_{2p}(q^2)]^2 d\xi = [F_{2p}(q^2)]^2.$$

Here the form factor of a single-particle harmonic oscillator wave function has the form

$$F_{nl}(q^2) = e^{-u/2} \sum_{\lambda=0}^{N_{\max}} \gamma_{\lambda}^{(nl)} (2u)^{\lambda} \tag{24}$$

with the dimensionless variable $u = q^2 b^2 / 2$ ($b = 2.434$ fm for Pb) and the coefficients $\gamma_{\lambda}^{(nl)}$ given in Table X. With entries $(n, l = 2, 1)$ of Table X the form factor squared

$$F_{2p}^2(q^2) = e^{-u} \left(1 - \frac{5}{3}u + \frac{17}{15}u^2 - \frac{31}{105}u^3 + \frac{9}{280}u^4 - \frac{1}{840}u^5 \right)^2,$$

defines the partial spin structure functions for ^{207}Pb in the simplest case (pure $2p_{1/2}$ neutron hole in the closed shell and $L = 0$).

Even though the probability of finding a pure $2p_{1/2}$ neutron hole in the $\frac{1}{2}^-$ ground state of ^{207}Pb is greater than 95%, the ground state magnetic moment is quenched due to the 1^+ p - h excitation involving the spin orbit partners. Hence, Kosmas and Vergados expected a similar suppression of the isovector spin matrix elements [48]. In this case for the $L = 0$ multipole one has

$$\Omega_{j=0,1}(\mathbf{q}) = (-1)^{j+1} C_0^2 \{ F_{2p}(q^2) / \sqrt{3} - 8 [(7/13)^{1/2} C_1 F_{0i}(q^2) + (-1)^j (5/11)^{1/2} C_2 F_{0h}(q^2)] \}.$$

TABLE X: The coefficients $\gamma_\lambda^{(nl)}$, entering into the polynomial describing the form factor (24) of a single particle harmonic oscillator wave function up to $6\hbar\omega$. From [77].

| $n l$ | $\lambda = 0$ | $\lambda = 1$ | $\lambda = 2$ | $\lambda = 3$ | $\lambda = 4$ | $\lambda = 5$ | $\lambda = 6$ |
|-------|---------------|---------------|---------------|---------------|---------------|---------------|---------------|
| 0 0 | 1 | | | | | | |
| 0 1 | 1 | -1/6 | | | | | |
| 1 0 | 1 | -1/3 | 1/24 | | | | |
| 0 2 | 1 | -1/3 | 1/60 | | | | |
| 1 1 | 1 | -1/2 | 11/120 | -1/240 | | | |
| 0 3 | 1 | -1/2 | 1/20 | -1/840 | | | |
| 2 0 | 1 | -2/3 | 11/60 | -1/60 | 1/1920 | | |
| 1 2 | 1 | -2/3 | 19/120 | -11/840 | 1/3360 | | |
| 0 4 | 1 | -2/3 | 1/10 | -1/210 | 1/15120 | | |
| 2 1 | 1 | -5/6 | 17/60 | -31/840 | 9/4480 | -1/26880 | |
| 1 3 | 1 | -5/6 | 29/120 | -47/1680 | 37/30240 | -1/60480 | |
| 0 5 | 1 | -5/6 | 1/6 | -1/84 | 1/3024 | -1/332640 | |
| 3 0 | 1 | -1 | 17/40 | -31/420 | 27/4480 | -1/4480 | 1/322560 |
| 2 2 | 1 | -1 | 2/5 | -1/15 | 41/8064 | -1/5760 | 1/483840 |
| 1 4 | 1 | -1 | 41/120 | -1/20 | 1/315 | -1/11880 | 1/1330560 |
| 0 6 | 1 | -1 | 1/4 | -1/42 | 1/1008 | -1/55440 | 1/8648640 |

With $C_0 = 0.973350$, $C_1 = 0.005295$, $C_2 = -0.006984$, definitions (23) and (24) one can calculate partial structure functions again. The situation with the multipole $L = 2$ contribution is more complicated, this contribution appears to be rather significant especially for the large momentum transfer (the details can be found in [48]). The complete ^{207}Pb partial structure

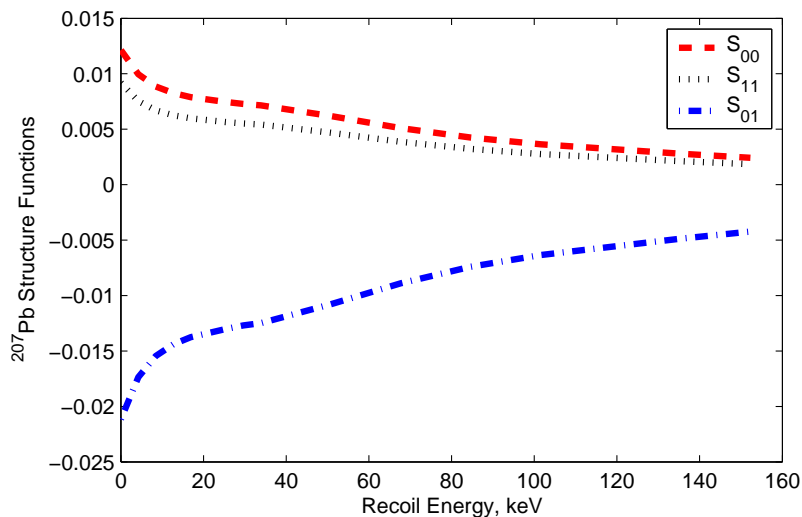


FIG. 12: Recoil energy dependence of the complete ^{207}Pb partial structure functions S_{ij}^{207} from (22) of Kosmas and Vergados [48].

functions S_{ij}^{207} from (22) of Kosmas and Vergados [48] is given in Fig. 12 as a function of the recoil energy.

Concluding the discussion of lead structure functions we note, following [48], that for a heavy nucleus and a high WIMP mass the momentum transfer dependence of the spin monopole ($L = 0$) matrix elements is quite large. It is, however, to a large extent neutralized by the spin quadrupole ($L = 2$). Thus the overall effect is not dramatic for WIMP masses less than 100 GeV. For the spin-induced cross section of heavy odd-A nuclear targets, as in the case of ^{207}Pb , the reduction is less pronounced since the high multipoles tend to enhance the cross section as the momentum transfer increases (for LSP mass < 200 GeV) and partially cancel the momentum reduction [48].

III. ON DATA ANALYSIS IN FINITE MOMENTUM TRANSFER FRAMEWORK

To perform the data analysis in the finite momentum transfer approximation directly in terms of the effective spin nucleon couplings $a_{0,1}$ together with the scalar WIMP-proton cross section $\sigma_{\text{SI}}^p(0)$ we propose to use formulas schematically given below. Nowadays it is also rather reasonable to assume $\sigma_{\text{SI}}^p(0) \approx \sigma_{\text{SI}}^n(0)$. The differential event rate (1) can be presented as follows:

$$\begin{aligned} \frac{dR(\epsilon, \varepsilon)}{dE_{\text{R}}} &= \mathcal{N}(\epsilon, \varepsilon, E_{\text{R}}, m_{\chi}) \left[\eta_{\text{SI}}(E_{\text{R}}, m_{\chi}) \sigma_{\text{SI}}^p + \eta'_{\text{SD}}(E_{\text{R}}, m_{\chi}, \omega) a_0^2 \right]; \quad (25) \\ \mathcal{N}(\epsilon, \varepsilon, E_{\text{R}}, m_{\chi}) &= \left[N_T \frac{c\rho_{\chi}}{2m_{\chi}} \frac{M_A}{\mu_p^2} \right] \frac{4\mu_A^2}{\langle q_{\text{max}}^2 \rangle} \langle \frac{v}{c} \rangle I(E_{\text{R}}) \theta(E_{\text{R}} - \epsilon) \theta(\varepsilon - E_{\text{R}}), \\ \eta_{\text{SI}}(E_{\text{R}}, m_{\chi}) &= \left\{ A^2 F_{\text{SI}}^2(E_{\text{R}}) \right\}; \\ \eta'_{\text{SD}}(E_{\text{R}}, m_{\chi}, \omega) &= \mu_p^2 \left\{ \frac{4}{2J+1} \left(S_{00}(q) + \omega^2 S_{11}(q) + \omega S_{01}(q) \right) \right\}; \\ I(E_{\text{R}}) &= \int_0^{\infty} \frac{\langle v^2 \rangle}{\langle v \rangle} \frac{dv}{v} f(v) \theta(4\mu_A^2 v^2 - 2M_A E_{\text{R}}). \end{aligned}$$

Here $\langle q_{\text{max}}^2 \rangle = 4\mu_A^2 \langle v^2 \rangle$ where $\langle v \rangle$ and $\langle v^2 \rangle$ are the mean and the mean squared velocity of WIMPs. The isovector-to-isoscalar nucleon couplings ratio is $\omega = a_1/a_0$. In expressions (25) are introduced the detector threshold recoil energy ϵ and the maximal available recoil energy ε ($\epsilon \leq E_{\text{R}} \leq \varepsilon$). In practice, for example with an ionization or scintillation signal, one has to take into account the quenching of the recoil energy, when visible recoil energy is smaller than the real recoil energy transmitted by the WIMP to the target nucleus.

Formulas (25) allow experimental recoil spectra to be directly described in terms of only *three* [3] independent parameters (σ_{SI}^p , a_0^2 and ω) for any fixed WIMP mass m_{χ} (and any neutralino

composition). Contrary to some other possibilities (see, for example, [43]), this procedure is direct and uses as much as possible the results of the most accurate nuclear spin structure calculations.

IV. CONCLUSION

There is continuous theoretical and experimental interest in existence of dark matter of the Universe. One of the best motivated non-baryonic dark matter candidates is the neutralino, the lightest supersymmetric particle. The motivation for supersymmetry arises naturally in modern theories of particle physics. In this work we discussed the spin-dependent interaction of neutralinos with odd- A nuclei. The nuclear structure plays an important role in determining the strength of the neutralino-nucleus cross section for this type of interaction and therefore defines the sensitivity of dark matter detection. In the limit of zero momentum transfer the relevant physical quantities are the proton and neutron spin averages $\langle \mathbf{S}_{p(n)} \rangle$, which have to be evaluated within a proper nuclear model. These values determine the event rate expected in a direct dark matter search experiment due to spin-dependent neutralino-nucleus interaction. In our previous paper [7] the calculations of zero-momentum transfer spin-dependent matrix elements was reviewed and to our knowledge, a complete list of calculated spin matrix elements was presented for nuclei throughout the periodic table [80]. The general feature is that spin matrix elements depend in general rather sensitively on the details of the nuclear structure. For a rather heavy WIMP (or light supersymmetric particle) and sufficiently heavy nuclei, the dependence of the nuclear matrix elements on the momentum transfer cannot be ignored. This affects the spin matrix elements.

A comprehensive collection, to our knowledge, of the spin-dependent structure functions $S^A(q)$ calculated for finite momentum transfer ($q > 0$) within different nuclear models is presented and discussed. These functions describe recoil energy dependence of the differential event rate due to spin-dependent neutralino-nucleon interaction, provided neutralino is a dark matter particle. Together with our previous paper “Nuclear spin structure in dark matter search: The zero momentum transfer limit” [7] this paper completes our review of the nuclear spin structure calculations involved in the problem of direct dark matter search.

Now that spin structure functions are available for almost all experimentally interesting nuclei (and collected in this review), they could be coherently used by all experimental groups.

This will make easier and more reliable comparisons between results of different dark matter search experiments and put it on the equal footing [41]. It will also allow one to reduce significantly the nuclear physics systematic uncertainties in the analysis of the data.

This work was supported in part by the VEGA Grant Agency of the Slovak Republic under contract No. 1/0249/03 and by the Russian Foundation for Basic Research (grant 06–02–04003). V.A.B. thanks V.A. Kuzmin (JINR) for careful reading of the manuscript and his comments concerning the maximal momentum transfer.

APPENDIX

For completeness, in this appendix we collect some formulas which allow one to connect the WIMP-nucleon scattering with the WIMP-nuclear scattering. We directly follow Engel et al. [1, 39]. The low-energy effective WIMP-nucleon Lagrangian is $\mathcal{L}_{\text{eff}} = \bar{\chi}\gamma^\mu\gamma_5\chi \cdot \mathcal{J}_\mu(x)$, where $\mathcal{J}_\mu(x) \propto \bar{N}\gamma_\mu\gamma_5N$ is the nucleon current. The one-nucleon matrix element of the current at finite q takes the approximate form

$$\langle p, s | \mathcal{J}_\mu(x) | p', s' \rangle = \bar{U}_N(p, s) \left(\frac{a_0 + a_1\tau_3}{2} \gamma_\mu\gamma_5 + \frac{m_N a_1 \tau_3}{q^2 + m_\pi^2} q_\mu \gamma_5 \right) U_N(p', s') e^{iq^\nu x_\nu}. \quad (26)$$

Here $q_\mu = p_\mu - p'_\mu$, $U_N(p, s)$ is the nucleon 4-component spinor and the energy transfer q_0 was assumed to be very small. In the nonrelativistic limit the time component of current (26) is proportional to $v/c \approx 10^{-3}$ and can be safely neglected. For the spatial component of the current one has the expression

$$\langle p, s | \vec{\mathcal{J}}_\mu(x) | p', s' \rangle = \langle s | \frac{a_0 + a_1\tau_3}{2} \vec{\sigma} - \frac{(\vec{\sigma} \cdot \vec{q}) a_1 \tau_3}{2(q^2 + m_\pi^2)} \vec{q} | s' \rangle e^{iq^\nu x_\nu} \quad (27)$$

where $|s\rangle$ and $|s'\rangle$ are two-component spinors. To obtain the cross section for scattering of the WIMP from nuclei one must evaluate the matrix element of the nucleon current between many-nucleon states. In the impulse approximation the cross section is

$$\frac{d\sigma^A}{dq^2}(v, q^2) = \frac{|\mathcal{M}|^2}{v^2(2J+1)\pi}, \quad \mathcal{M} = \langle s | \vec{\sigma}_\chi | s' \rangle \int d^3x \langle J, M | \mathcal{J}(\vec{x}) | J, M' \rangle \times e^{i\vec{q}\cdot\vec{x}}, \quad (28)$$

where $|\mathcal{M}|^2$ is summed over s, s', M, M' . Here J is the angular momentum of the ground state and the nuclear current $\mathcal{J}(\vec{x})$ is given by the sum over all nucleons with current matrix elements

from (27). Expanding the current in vector spherical harmonics one obtains the form given in (2) and (3):

$$\frac{d\sigma_{\text{SD}}^A}{dq^2}(v, q^2) = \frac{S_{\text{SD}}^A(q^2)}{v^2(2J+1)}, \quad S_{\text{SD}}^A(q)y = \sum_{L \text{ odd}} (|\langle N || \mathcal{T}_L^{\text{el}5}(q) || N \rangle|^2 + |\langle N || \mathcal{L}_L^5(q) || N \rangle|^2).$$

The transverse electric $\mathcal{T}^{\text{el}5}(q)$ and longitudinal $\mathcal{L}^5(q)$ multipole projections of the axial vector current operator are given by (see [1, 39, 40, 41] for details):

$$\begin{aligned} \mathcal{T}_L^{\text{el}5}(q) &= \frac{1}{\sqrt{2L+1}} \sum_i^A \frac{a_0 + a_1 \tau_3^i}{2} \left[-\sqrt{L} M_{L,L+1}(q\vec{r}_i) + \sqrt{L+1} M_{L,L-1}(q\vec{r}_i) \right], \\ \mathcal{L}_L^5(q) &= \frac{1}{\sqrt{2L+1}} \sum_i^A \left(\frac{a_0}{2} + \frac{a_1 m_\pi^2 \tau_3^i}{2(q^2 + m_\pi^2)} \right) \left[\sqrt{L+1} M_{L,L+1}(q\vec{r}_i) + \sqrt{L} M_{L,L-1}(q\vec{r}_i) \right], \end{aligned}$$

where $M_{L,L'}(q\vec{r}_i) = j_{L'}(qr_i) [Y_{L'}(\hat{r}_i) \vec{\sigma}_i]^L$, m_π is the pion mass and $a_{0(1)}$ is the isoscalar (isovector) effective spin-dependent WIMP-nucleon coupling. For example, the above-mentioned matrix elements one can calculate within the harmonic oscillator approach on the basis of results given in [78].

-
- [1] *Engel J.* // Phys. Lett. B. 1991. V.264. P.114–119.
 - [2] *Bottino A., Donato F., Fornengo N., and Scopel S.* // hep-ph/0307303.
 - [3] *Bednyakov V. A., Klapdor-Kleingrothaus H. V., and Kovalenko S. G.* // Phys. Lett. B. 1994. V.329. P.5–9, hep-ph/9401271.
 - [4] *Bednyakov V. A. and Klapdor-Kleingrothaus H. V.* // Phys. Rev. D. 2001. V.63. P.095005, hep-ph/0011233.
 - [5] *Bednyakov V. A.* // Phys. Atom. Nucl. 2003. V.66. P.490–493, hep-ph/0201046.
 - [6] *Bednyakov V. A.* // Phys. Atom. Nucl. 2004. V.67. P.1931–1941, hep-ph/0310041.
 - [7] *Bednyakov V. A. and Simkovic F.* // Phys. Part. Nucl. 2005. V.36. P.131–152, hep-ph/0406218.
 - [8] *Bednyakov V. A. and Klapdor-Kleingrothaus H. V.* // hep-ph/0504031.
 - [9] *Girard T. A. et al.* // Phys. Lett. B. 2005. V.621. P.233–238, hep-ex/0505053.
 - [10] *Girard T. A. et al.* // hep-ex/0504022.
 - [11] *Giuliani F.* // Phys. Rev. Lett. 2004. V.93. P.161301, hep-ph/0404010.
 - [12] *Giuliani F. and Girard T. A.* // Phys. Rev. D. 2005. V.71. P.123503, hep-ph/0502232.
 - [13] *Savage C., Gondolo P., and Freese K.* // Phys. Rev. D. 2004. V.70. P.123513, astro-ph/0408346.
 - [14] *Benoit A. et al.* // Phys. Lett. B. 2005. V.616. P.25–30, astro-ph/0412061.
 - [15] *Tanimori T. et al.* // Phys. Lett. B. 2004. V.578. P.241–246, astro-ph/0310638.
 - [16] *Ovchinnikov B. M. and Parusov V. V.* “The preparing of an experiment for search the spin-dependent interactions of wimp.” // INR preprint 1097/2003, 2003.
 - [17] *Moulin E., Mayet F., and Santos D.* // Phys. Lett. B. 2005. V.614. P.143–154, astro-ph/0503436.

- [18] *Mayet F., Santos D., Bunkov Y. M., Collin E., and Godfrin H.* // Phys. Lett. B. 2002. V.538. P.257, astro-ph/0201097.
- [19] *Klapdor-Kleingrothaus H. V., Krivosheina I. V., and Tomei C.* // Phys. Lett. B. 2005. V.609. P.226–231.
- [20] *Alner G. J. et al.* // Nucl. Instrum. Meth. A. 2004. V.535. P.644–655.
- [21] *Snowden-Ifft D. P., Martoff C. J., and Burwell J. M.* // Phys. Rev. D. 2000. V.61. P.101301, astro-ph/9904064.
- [22] *Gaitskell R. J. et al.* // Nucl. Instrum. Meth. A. 1996. V.370. P.162–164.
- [23] *Sekiya H., Minowa M., Shimizu Y., Sukanuma W., and Inoue Y.* // astro-ph/0405598.
- [24] *Morgan B., Green A. M., and Spooner N. J. C.* // Phys. Rev. D. 2005. V.71. P.103507, astro-ph/0408047.
- [25] *Vergados J. D.* // Part. Nucl. Lett. 2001. V.106. P.74–108, hep-ph/0010151.
- [26] *Vergados J. D.* // Phys. Atom. Nucl. 2003. V.66. P.481–489, hep-ph/0201014.
- [27] *Jungman G., Kamionkowski M., and Griest K.* // Phys. Rept. 1996. V.267. P.195–373, hep-ph/9506380.
- [28] *Divari P. C., Kosmas T. S., Vergados J. D., and Skouras L. D.* // Phys. Rev. C. 2000. V.61. P.054612.
- [29] *Bednyakov V. A., Klapdor-Kleingrothaus H. V., and Kovalenko S. G.* // Phys. Rev. D. 1997. V.55. P.503–514, hep-ph/9608241.
- [30] *Bernabei R. et al.* // Phys. Lett. B. 2000. V.480. P.23–31.
- [31] *Bernabei R. et al.* // Riv. Nuovo Cim. 2003. V.26. P.1–73, astro-ph/0307403.
- [32] *Bernabei R. et al.* // astro-ph/0311046.
- [33] *Lewin J. D. and Smith P. F.* // Astropart. Phys. 1996. V.6. P.87–112.
- [34] *Smith P. F. and Lewin J. D.* // Phys. Rept. 1990. V.187. P.203.
- [35] *Bednyakov V. A. and Klapdor-Kleingrothaus H. V.* // Phys. Atom. Nucl. 1999. V.62. P.966–974.
- [36] *Bednyakov V. A., Kovalenko S. G., and Klapdor-Kleingrothaus H. V.* // Phys. Atom. Nucl. 1996. V.59. P.1718–1727.
- [37] *Bednyakov V. A., Kovalenko S. G., Klapdor-Kleingrothaus H. V., and Ramachers Y.* // Z. Phys. A. 1997. V.357. P.339–347, hep-ph/9606261.
- [38] *Bednyakov V. A., Klapdor-Kleingrothaus H. V., and Kovalenko S.* // Phys. Rev. D. 1994. V.50. P.7128–7143, hep-ph/9401262.
- [39] *Engel J., Pittel S., and Vogel P.* // Int. J. Mod. Phys. 1992. V.E1. P.1–37.
- [40] *Ressell M. T. et al.* // Phys. Rev. D. 1993. V.48. P.5519–5535.
- [41] *Ressell M. T. and Dean D. J.* // Phys. Rev. C. 1997. V.56. P.535–546, hep-ph/9702290.
- [42] *Engel J., Ressell M. T., Towner I. S., and Ormand W. E.* // Phys. Rev. C. 1995. V.52. P.2216–2221, hep-ph/9504322.
- [43] *Tovey D. R., Gaitskell R. J., Gondolo P., Ramachers Y., and Roszkowski L.* // Phys. Lett. B. 2000. V.488. P.17–26, hep-ph/0005041.
- [44] *Vergados J. D.* // J. Phys. G. 1996. V.22. P.253–272, hep-ph/9504320.
- [45] *Dimitrov V., Engel J., and Pittel S.* // Phys. Rev. D. 1995. V.51. P.291–295, hep-ph/9408246.
- [46] *Engel J., Pittel S., Ormand E., and Vogel P.* // Phys. Lett. B. 1992. V.275. P.119–123.
- [47] *Nikolaev M. A. and Klapdor-Kleingrothaus H. V.* // Z. Phys. A. 1993. V.345. P.183–186.
- [48] *Kosmas T. S. and Vergados J. D.* // Phys. Rev. D. 1997. V.55. P.1752–1764, hep-ph/9701205.
- [49] *Pacheco A. F. and Strottman D.* // Phys. Rev. D. 1989. V.40. P.2131–2133.

- [50] *Iachello F., Krauss L. M., and Maino G.* // Phys. Lett. B. 1991. V.254. P.220–224.
- [51] *Ellis J. R. and Flores R. A.* // Nucl. Phys. B. 1988. V.307. P.883.
- [52] *Ellis J. R. and Flores R. A.* // Phys. Lett. B. 1991. V.263. P.259–266.
- [53] *Engel J. and Vogel P.* // Phys. Rev. D. 1989. V.40. P.3132–3135.
- [54] *Ogawa I. et al.* // Nucl. Phys. A. 2000. V.663. P.869–872.
- [55] *Boukhira N. et al.* // Nucl. Phys. Proc. Suppl. 2002. V.110. P.103–105.
- [56] *Takeda A. et al.* // Phys. Lett. B. 2003. V.572. P.145–151, astro-ph/0306365.
- [57] *Miuchi K. et al.* // Astropart. Phys. 2003. V.19. P.135–144, astro-ph/0204411.
- [58] *Brown B. and Wildenthal B.* // At. Data Nucl. Data Tab. 1985. V.33. P.347.
- [59] *Brown B. and Wildenthal B.* // Ann. Rev. Nucl. Part. Sci. 1988. V.38. P.29.
- [60] *Bernabei R. et al.* // Nucl. Phys. A. 2003. V.719. P.257–265.
- [61] *Ahmed B. et al.* // Astropart. Phys. 2003. V.19. P.691–702, hep-ex/0301039.
- [62] *Cebrian S. et al.* // Nucl. Phys. Proc. Suppl. 2003. V.114. P.111–115, hep-ex/0211050.
- [63] *Yoshida S. et al.* // Nucl. Phys. Proc. Suppl. 2000. V.87. P.58–60.
- [64] *Angloher G. et al.* // Phys. Atom. Nucl. 2003. V.66. P.494–496.
- [65] *Resler D. and Grimes S.* // Computers in Phys. 1988. V.2 (3). P.65–66.
- [66] *Klapdor-Kleingrothaus H. V. et al.* // Astropart. Phys. 2003. V.18. P.525–530, hep-ph/0206151.
- [67] *Petrovich F., McManus H., Madsen V., and Atkinson J.* // Phys. Rev. Lett. 1969. V.38. P.895.
- [68] *Dimitrov V.* // Phys. Rev. C. 1994. V.50. P.2893–2899.
- [69] *Nikolaev M. A. and Klapdor-Kleingrothaus H. V.* // Z. Phys. A. 1993. V.345. P.373–376.
- [70] *Hjorth-Jensen M., Kuo T. T. S., and Osnes E.* // Phys. Rept. 1995. V.261. P.125–270.
- [71] *Stoks V. G. J., Klomp R. A. M., Terheggen C. P. F., and de Swart J. J.* // Phys. Rev. C. 1994. V.49. P.2950–2962, nucl-th/9406039.
- [72] *Hart S. P.* // Nucl. Phys. Proc. Suppl. 2002. V.110. P.91–93.
- [73] *Luscher R.* // astro-ph/0305310.
- [74] *Bernabei R. et al.* // Nucl. Phys. Proc. Suppl. 2002. V.110. P.88–90.
- [75] *Vergados J. D. and Kosmas T. S.* // hep-ph/9701204.
- [76] *Vergados J. D. and Kosmas T. S.* // hep-ph/9701206.
- [77] *Kosmas T. S. and Vergados J. D.* // nucl-th/9509026.
- [78] *Donnelly T. and Haxton W.* // At. Data Nucl. Dat. Tab. 1979. V.23. P.103–176.
- [79] In Table 6 of [7] these values should correspond to the large shell-model spaces.
- [80] In Table 4 of [7] the results for ^{43}Ca ($J = 7/2$) [33] were missed — one has $\langle \mathbf{S}_n^{43} \rangle = 0.5$ in ISPSM and $\langle \mathbf{S}_n^{43} \rangle = 0.344$ ($\mu = -1.318\mu_N$) in OGM together with $\langle \mathbf{S}_p^{43} \rangle \equiv 0$.